KfK 4038
Mai 1987

Experiments and Correlations of Pressure Loss Coefficients for Hexagonal Arranged Rod Bundles (P/D > 1.02) with Helical Wire Spacers in Laminar and Turbulent Flows

K. Marten, S. Yonekawa, H. Hoffmann
Institut für Reaktorbauelemente
Projekt Schneller Brüter
Projektgruppe LWR-Sicherheit

Kernforschungszentrum Karlsruhe

KERNFORSCHUNGSZENTRUM KARLSRUHE
INSTITUT FÜR REAKTORBAUELEMENTE
PROJEKT SCHNELLER BRÜTER
PROJEKTGRUPPE LWR-SICHERHEIT

KfK 4038

EXPERIMENTS AND CORRELATIONS OF PRESSURE LOSS COEFFICIENTS FOR HEXAGONAL ARRANGED ROD BUNDLES (P/D > 1.02) WITH HELICAL WIRE SPACERS IN LAMINAR AND TURBULENT FLOWS.

K. Marten, S. Yonekawa *, H. Hoffmann

*) Present address: PNC, Ningyo Pass Works, Japan

Kernforschungszentrum Karlsruhe GmbH, Karlsruhe

Kernforschungszentrum Karlsruhe GmbH
Postfach 3640, 7500 Karlsruhe 1

ISSN 0303-4003

EXPERIMENTS AND CORRELATIONS OF PRESSURE LOSS COEFFICIENTS FOR HEXAGONAL ARRANGED ROD BUNDLES (P/D > 1.02) WITH HELICAL WIRE SPACERS IN LAMINAR AND TURBULENT FLOWS.

Abstract

Advanced pressurized water reactors as well as sodium cooled fast reactors, in their breeding and absorber elements, use tightly packed rod bundles with hexagonally arranged rods. Helical wires or helical fins serve as spacers.

The pressure loss coefficients of twelve bundles with helical wires were determined systematically in water experiments under the following characteristic conditions:

Reynolds number range	$50 < Re < 90{,}000$.
Pitch-to-diameter ratios	$1.02 < P/D < 1.10$.
Helical-lead-to-rod-diameter ratios	$8.3 < H/D < 16.7$.

High measuring accuracy was achieved by very precise fabrication of the bundles and the shroud as well as by investigations of the proper measuring techniques. The results show a dependency of the loss coefficients on the Reynolds number and on the P/D and H/D ratios of the bundles. These results together with available systematic experimental results of investigations at P/D > 1.1 were used to develop a correlation to determine the pressure loss coefficients of tightly and widely packed hexagonally arranged rod bundles with helical wire spacers under laminar and turbulent flow conditions. These correlations were used to recalculate and compare results of pressure loss investigations found in the literature; good agreement was demonstrated. Hence, calculation methods exist for a broad range of applications to determine the pressure loss coefficients of hexagonally arranged rod bundles with helical wires for spacers.

EXPERIMENTE UND KORRELATIONEN FÜR DRUCKVERLUSTBEIWERTE VON BÜNDELN MIT HEXAGONALER STABANORDNUNG (P/D > 1.02) UND WENDELDRAHT-ABSTANDSHALTERN BEI LAMINARER UND TURBULENTER STRÖMUNG.

Kurzfassung:

Für Brennelemente eines fortgeschrittenen Druckwasserreaktors sowie Brut- und Absorberelemente von schnellen natriumgekühlten Reaktoren werden Bündel mit engen Stabpackungen benötigt, die hexagonale Stabanordnungen aufweisen. Zur Abstandshalterung im Bündelverbund dienen vorwiegend Drähte oder Rippen.

Duckverlustbeiwerte von 12 Bündeln mit Drahtabstandshalter wurden für folgende Parameter systematisch in Wasserströmung ermittelt:

Reynolds-Zahlen:	$50 < Re < 90{,}000.$
Stababstandsverhältnisse:	$1.02 < P/D < 1.10.$
Steigungsverhältnisse:	$8.3 < H/D < 16.7.$

Die Druckverlustbeiwerte zeigen im laminaren wie im turbulenten Strömungsbereich eine Abhängigkeit von den P/D- und H/D-Verhältnissen sowie von den Reynolds-Zahlen. Eine hohe Genauigkeit der Meßergebnisse wurde durch präzise Herstellung der Bündel und des Kastens sowie durch Untersuchungen zur geeigneten Meßtechnik erreicht.

Unter Einbeziehung von Ergebnissen aus systematischen Druckverlust-Untersuchungen an Bündeln mit weiten Stabpackungen wurden Korrelationen zur Berechnung der Druckverlustbeiwerte für laminare und turbulente Strömung erstellt. Diese Korrelationen wurden zusätzlich an in der Literatur verfügbaren Einzelergebnissen getestet. Die Übereinstimmung von Meß- und Rechenwerten ist gut. Damit sind für einen weiten Anwendungsbereich Beziehungen verfügbar zur Bestimmung der Druckverluste von Bündeln mit Wendeldraht-Abstandshaltern.

CONTENT

1. PROBLEM

Bundles with tight rod packings are required for the fuel elements of advanced pressurized water reactors and for the breeding and absorber elements of sodium cooled fast reactors. Hexagonal rod arrays are selected for tight rod packings. Mainly wires or fins are used as spacers between the rods within bundle arrays. A bundle with a hexagonal rod array and wires used for spacers is shown in Fig. 1. The wires are wound helically on all rods at the same pitch angles and in the same directions.

Systematic measurements of pressure loss coefficients have so far been carried out only on bundles with wire spacers for the range of $1.13 < P/D < 1.42$; $8.33 < H/D < 50$, and $1200 < Re < 300{,}000$ /1/. A correlation with the experimental results has been found for computation of the pressure loss coefficients, which also applies to certain bundles with multiple-course fins as spacers /2; 3/. Consequently, the pressure loss in a bundle is determined mainly by the Reynolds number and by the dimensionless quantities, P/D, H/D. Figure 2 is a plot of the range of pressure loss coefficients, $\lambda = f(P/D)$, investigated so far for a Reynolds number of $Re = 3 \times 10^4$. For the range of tight rod packings, $P/D < 1.13$ (hatched area), only very few measured results are known from the literature, and these do not correlate with each other. In order to establish an empirical relation for calculation of the pressure loss coefficients for tight rod packings ($P/D < 1.13$) for practical applications, systematic measurements were performed for the following experimental parameters:

Rod pitch-to-diameter ratio, P/D:	1.02; 1.04; 1.07; 1.1
Helical lead-to-diameter ratio, H/D:	8.3; 12.5; 16.7
Number of rods, Z:	37
Reynolds numbers in the bundle:	$50 < Re < 90{,}000$

First measured results obtained in these studies for the turbulent and laminar flow regime have been communicated in /4/, /5/ and /6/. This report is a summary of all findings and a comparison of the correlations developed on this basis with findings also by other authors.

2. EXPERIMENT

2.1 Precision Requirements

In analogy to the relation pertaining to the circular tube, the irreversible pressure loss of a bundle with helical wire spacers is described as follows:

$$\Delta p = \lambda \, (L/d_h) \, \bar{u}^2 \quad \rho/2 \tag{1}$$

Hydraulic diameter : $d_h = 4 \; A/U$ (2)

Fluid velocity in the bundle: $\bar{u} = \dot{V}/A$ (3)

With Equations (2) and (3) the pressure loss coefficient is calculated according to (1) as

$$\lambda = 8 \;\; \Delta p \;\; A^3/(L \, \rho \; U \; \dot{V}^2) \tag{4}$$

In accordance with the similarity principles, the following dependency applies to the pressure loss coefficient for a hydraulic, isothermal flow:
$\lambda = f(Re;\ P/D;\ H/D;\ D/\varepsilon;\ Z)$

The Reynolds number is

$$Re = \bar{u} \;\; d_h/\nu \tag{5}$$

or, with Equations (2) and (3):

$$Re = 4 \; \dot{V}/(\nu \, U) \tag{6}$$

An error assessment was made in order to find out which differences in the measured quantities have the greatest influence on the maximum error of the quantities to be determined. The maximum error, Δy, for the functional quantitity is calculated as follows in accordance with the propagation of single errors, Δx:
$\Delta y = (\partial f/\partial x_1)\Delta x_1 + \ldots\ldots (\partial f/\partial x_n)\Delta x_n$

In the application to the equations determining the pressure loss coefficients (4) and the Reynolds number (5), the maximum relative error is calcu-

lated as

$$\Delta\lambda/\lambda = |\Delta(\Delta p)/\Delta p| + 3|\Delta A/A| + 2|\Delta\dot{V}/\dot{V}| + |\Delta U/U| + |\Delta L/L| + |\Delta\rho/\rho| \qquad (7)$$

$$\Delta Re/Re = |\Delta\dot{V}/\dot{V}| + |\Delta\nu/\nu| + |\Delta U/U| \qquad (8)$$

The relative error in the pressure loss coefficient consequently is influenced most strongly by inaccuracies in the flow cross section, A, of the bundle. As the flow cross section results from the inner cross section of the shroud minus the cross sectional areas of the rods and the wires, the relative errors are calculated as follows:

$$\Delta A/A = (|\Delta A_K| + |\Delta A_{St}| + |\Delta A_{Dr}|)/(A_K-(A_{St}+A_{Dr})) \qquad (9)$$

For Equation (9) this means that for an unchanged cross sectional area of the shroud the relative error in the flow cross section rises with decreasing rod pitch-to-diameter ratio while the tolerances in the rods and the wires remain unchanged. The relative error in the flow cross section tribles with the change in the P/D ratio from 1.35 to 1.02. For this reason, the tolerances in fabricating the bundle geometry were kept as narrow as possible for tight rod packings, as is shown in Table 1. According to Equation (9), this results in a relative error in the flow cross section of only $\pm$ 1.0 % for the lowest value of P/D = 1.02.

The maximum possible error for the pressure loss coefficients to be determined was calculated to be $\pm$ 5 % according to Equation (7) and $\pm$ 2 % for the Reynolds number according to Equation (8). The maximum possible errors underlying these calculations are summarized in Table 2. They apply to the turbulent flow regime in the bundle ($Re\sqrt{F} < 19{,}000$). In the laminar flow regime pressure drops in the range of 20 - 800 Pa and volume flows of $(0.03 - 0.45)\ 10^{-3}\ m^3/s$ must be measured. The high measuring accuracies indicated cannot be attained in this way; consequently the maximum possible error in determining the pressure loss coefficient must be assumed at least to double.

2.2 Test Setup

Because of the stringent precision requirements to be met by the bundle geo-

metry, only one shroud for all bundles was made for cost reasons. The rod diameters, however, were varied in accordance with the rod pitch-to-diameter ratios. The shroud (Fig. 3) was made out of two identical half shells sealed at the seams with a circular cord packing. This allowed precise fabrication of the hexagonal cross section at a minimum of expense, and also made for simple and easy assembly of the bundles without affecting the position and form of the thin spacer wires on the rods. Six pressure tap bores in one cross sectional plane constituted one measuring plane. Several measuring planes were installed along the shroud. The distance from the inlet to the first measuring plane was 500 mm for a shroud length of 1500 mm (Fig. 5a). At the inlet and the outlet of the shroud the rods were fixed in spark eroded lattice type spacers so that, on the one hand, the spacer wires in one cross sectional plane were always in the same direction relative to the rods and, on the other hand, the rod pitch-to-diameter ratio was maintained at the ends of the bundle. A photograph of a complete bundle in the bottom half shell of the shroud is shown in Fig. 4. The wires were wound on the rods helically by means of a special system and immobilized by spot welding every quarter turn. The dimensions, tolerances, and surface qualities of shroud, rods and wires are listed in Table 1.

2.3 Measuring Systems

Pressure loss Measurements - Measuring Methods

In a hexagonal rod bundle with helical wire spacers a helical flow is produced between the outer row of the rods in the bundle and the shroud /2/. This flow generates a sinusoidal pressure distribution at the shroud walls of a cross sectional plane /7/. A large variety of measuring techniques were studied for precise, and yet simple, measurement of the pressure loss in the bundle.

The standard of pressure loss measurements were examined with bundles characterized by $P/D = 1.07$, and $H/D = 8.3$ and 12.5. For these experiments first the original axial pressure measurement positions were used placed in the shroud at axial intervals of 125 mm (Fig. 5a). The bundle cross sections at these measurement positions reveal random orientations of the wire spacers with respect to the axis of the pressure measurement taps. In addition to these original axial pressure measurement positions new pressure measurement

positions were installed where the orientations of the wire spacers with respect to the tap axis was the same in each cross section (60^{o}, 180^{o}, 300^{o}). The helical pitch was H = 191 mm and this was also the distance between the axial measurement position 1 and 3, whilst 3 x H were realized between the axial positions 1 and 8.

At each axial measurement position six pressure measurement taps were installed. They could be used at single measuring devices each or as six interconnected devices to register an averaged value of the axial measuring position.

With these two kinds of pressure measurement tap locations (original, new), five different pressure drop measuring methods were examined. The measured pressure losses for each method was used to evaluate the friction factors as function of the Reynolds numbers. These friction factors were then intercompared with each other. The pressure loss measuring methods were:

Method 1: Pressure loss measurement using the original axial pressure measurement positions; all six pressure taps are interconnected and the orientation of the wire spacers is random at each axial position.

Method 2: Pressure loss measurement using the original pressure measurement positions; only one pressure tap is taken at each axial position at the same flat of the shroud. The orientation of the wire spacers is random at each used tap.

Method 3: Pressure loss measurement by new pressure measurement positions; all six pressure taps are interconnected and the orientation of the wire spacers is the same at each axial position.

Method 4: Pressure loss measurement by new pressure measurement positions; only one pressure tap is taken at each axial position, where the orientation of the wire spacers is the same at each used tap. For example, pressure loss between section 1 and 3 or 3 and 8 were measured (see Fig. 5a).

Method 5: Pressure loss measurement at the bundle inlet and outlet of two bundles with different lengths; all other geometrical conditions are the same.

In method 1 to 4 the friction factor is evaluated from the pressure drop measurement along a defined axial bundle length (Equation (4)).

Method 5 is completely different from methods 1 to 4. It was also used in /1/. It was taken to measure the pressure drops in bundles of P/D = 1.07, H/D = 8.3, differing in lengthes by 750 mm. Two bundles, shown in Fig. 5c, were set up and pressure measurement taps were placed away from the bundle at the inlet (upstream) and outlet (downstream) sections. In this case the influences of orientations of the wire spacers on the pressure measurement position could be avoided. When the two bundles' pressure drop are measured with the same temperature and the same flow rate, the friction factor can be evaluated from the measured overall pressure losses (ΔP) of the two bundles differing in lengths (L) using equation (1):

$$(\Delta P_1 - \Delta P_2) = \frac{\lambda (L_1 - L_2) \rho \bar{u}^2}{2 d_h} \tag{10}$$

$$\lambda = \frac{2 d_h (\Delta P_1 - \Delta P_2)}{\bar{u}^2 \rho (L_1 - L_2)} \tag{11}$$

The five different pressure measurement methods were investigated. In addition, the following influences on the pressure loss measurements were evaluated too with each measurement method:

- water temperature
- axial distances of pressure loss measuring positions
- circumferential positions of pressure loss measuring taps.

The results of these experiments were intercompared in the form of $\lambda = f(Re)$. Fig. 6a shows the results of method 1, 3 and 4. All data are within a deviation of $\pm$ 2 %. The dependences of the friction factors from the water temperature as well as from the axial measurement lengths were not detected.

When only one tap was taken at random orientations of the wire spacers at the measuring positions (method 2), data scatter about $\pm$ 6 % which is shown in Fig. 6b. The data were plotted for the six interconnected taps (method 1), and for method 2, where one measurement tap each along B; C and F-line of the hexagonal flats were used to evaluate the friction factors. From these results, the influence of the azimuthal pressure distribution along the shroud periphery can be deduced. The six connected taps method seems to average the pressure at each measuring position and this averaged values are not so wide-

ly different between random orientation of the wire spacers and the same orientation of the wire spacers at each measuring position.

Furthermore, method 5 was examined with the same bundle geometry of P/D = 1.07; H/D = 8.3 to reconfirm the correctness of method 1. This method contains no effect of sweeping flow produced by the wire spacers but it takes twice the measuring time as the above mentioned method 1. The result is shown in Fig. 6c. There is a good agreement between method 1 and 5. Finally method 1 can be adopted as the standard and easier method of pressure drop measurement for wire wrapped rod bundles. All measurements were therefore carried out following this procedure.

Flow Profile at the Bundle Entrance

Velocity profiles at the inlet of the test section were measured by Pitot tube to ensure homogeneous flow conditions across the inlet flow section, where a slug flow profile should be realized. For this reason the local velocities were measured by traversing a Pitot tube horizontal and vertical across the inlet tube diameter of 102 mm. Fig. 7 shows the measuring device and measured results. The measured local velocity is related to the averaged mean velocity ($u/\bar{u}$) and plotted versus the tube diameter. In addition the measured results are compared with the universal velocity law $u^+ = 5.5+2.5 \ln y^+$. The expected flow behavior can be seen, namely that with increasing Reynolds number, the velocity profile takes a flatter shape.

In general the results show a piston type velocity profile at the bundle entrance. The distance up to the first measuring plane is $L/d_h > 60$. Hence a fully developed bundle flow can be assumed.

Pressure Differences, Temperatures, Flowrate

The differential pressures (Δp) between the measuring planes were determined by means of U-tube pressure gages. This method was used as long as the differential pressure was beyond 300 Pa. Inductive and capacitive measuring systems were applied when the pressure differences were < 300 Pa. The capacitive measuring system was used below 125 Pa and calibrated with an Askania-minimeter allowing an accuracy of 1/100 mm H_2O columne. The fluid temperature (T) was measured by NTC resistance thermometers upstream and downstream of

the bundle. Oscillator flowmeters were used to determine the volume flow ($\dot{V}$). The measuring points are indicated in the water loop (Fig. 8). For the studies conducted at Reynolds numbers, $Re < 10^3$, the range of measurement of the smallest flowmeter installed was underrun. In this case, the water loop was opened and the volume flow determined by volume measurement over a period of 100 s.

2.4 Test Loop

The tests were conducted in water. For this purpose, the test section was installed in the water loop in a horizontal position. Figure 8 shows the loop. A variable-speed centrifugal pump circulated the water through a cooler to the test bundle and back into a feed tank equipped with an electric heater. The cooler and the heater were installed to achieve the wide range of Reynolds numbers in the bundle. Here are the data of the loop:

Volume flow: 0.4 - 100 m^3/h.
Max. pump pressure: 14 bar.
Fluid temperature: 15 - 80 ^oC.

3. RESULTS

3.1 Experimental Results

The pressure loss coefficients determined for the twelve bundles are shown as a function of the Reynolds number in Figs. 9-12. In addition, the numerical values are listed in Tables A1-A12 in the Annex. Each diagram indicates the results obtained for bundles with identical P/D ratios, but different H/D ratios. For a better survey the loss coefficients for bundles with different H/D ratios are multiplied by distinct factors (1λ; 2λ; 4λ). The figures show:

- The pressure loss coefficients drop as the Reynolds number rises.
- They increase with decreasing H/D ratio of the helical wire and increasing P/D ratio of the bundle at a constant Reynolds number (see also Fig. 14).
- For the bundles with the smallest rod pitch-to-diameter ratio P/D=1.02, the transition from laminar to turbulent bundle flows is clearly recognizable.

- For the bundles with the highest rod pitch-to-diameter ratio, P/D = 1.1 the transition region is not very pronounced.

The change from laminar to turbulent bundle flows is shown separately for the two bundles with P/D = 1.02 and P/D = 1.1 with identical H/D = 16.7 in Fig. 13. The reason for the clearly marked transition region at P/D = 1.02 is that with decreasing P/D ratios the projection areas of the channels (Fig. 1) become less obstructed by the spacers. Hence the main flow direction remains axisparallel to the rods and a bundle with small P/D ratio can therefore be compared with similar flow behavior of a surface with turbulence promoters. At large P/D ratios the projection area overlaps the channel cross section and the flow has to meander through the channels increasing the overall friction forces and explaining the undistinct transition region. For comparison the smooth tube data are also indicated /8/.

The pressure loss coefficients determined are shown in Fig. 14 as a function of the P/D ratio for the three helical wire ratios H/D at a constant Reynolds number, similar to Fig. 2, namely for the turbulent flow regime, Re = 30,000. In addition, also the experimental data from /1/ were plotted for the 37-rod bundles as well as measured data of P/D = 1 taken from /9/ and /10/. In order to verify the application of the familiar correlations according to /1/ also on the basis of the measured data available in this case, values were calculated outside the range of validity indicated in /1/, i.e., for P/D < 1.13, and indicated in the figure as extrapolated data (dotted line).

It can be concluded:

- The pressure loss coefficients rise
  - with increasing P/D ratio because of increasing blockage of the projection areas of the subchannels by the helical wires (Fig. 1), which results in increasing deflection of the subchannel flow from the axial main flow;
  - with decreasing H/D, because of the increasing inclination of the helical wires relative to the axial main flow connected with the increase in the number of flow deflections in that flow section.
- The pressure loss coefficients decrease more strongly with decreasing P/D ratio for low helical leads as the reduction of the gaps between the rods hardly permits any cross flow to develop and, for the axial bundle

flow, the helical wires in that case only act like turbulence promoters in the subchannel.

- The calculated pressure loss coefficients show unsatisfactory agreement with the measured data, especially for low H/D ratios, outside the range of validity of the correlations for P/D < 1.13.

3.2 Computed Results

3.2.1 Turbulent Flow

As the available correlation /1/ cannot be applied to calculations of pressure loss coefficients in tightly packed rod bundles, a new correlation had to be established. For this purpose, a computer program was developed /11/ to determine for the experimental data a functional dependence of the pressure loss coefficients, λ_R, on the Reynolds number, the P/D and the H/D ratios by means of the least squares of the deviations.

$$\lambda_R = f\ (Re;\ P/D;\ H/D;\ Z)$$

Data measured by the authors (Annex, Table A1-A12) and taken from /1/ were used to establish the correlation. Initially, the setups used to calculate the pressure loss coefficients were taken from /1/ without any modification. Consequently, it holds for the fully turbulent range
$(1.9 \times 10^4 < (Re\ \sqrt{F}) < 5 \times 10^5)$:

$$\lambda_R = 0{,}1317\ (Re\ \sqrt{F})^{-0{,}17}\ F\ G \qquad (12)$$

For the turbulent transitional range $(2 \times 10^3 < (Re\ \sqrt{F}) < 1.9 \times 10^4)$:

$$\lambda_R = (0{,}1317\ (Re\ \sqrt{F})^{-0{,}17} + (60/(Re\ \sqrt{F}) - 3{,}2\ \ 10^{-3})F\ \ G \qquad (13)$$

The factor G takes into account the ratio between the circumference of the shroud wall and the circumference of the bundle wall:

$$1/G = 1 + (U_K/U_B) \qquad (14)$$

For a bundle of infinite extension, the factor G = 1. Calculating the wetted perimeter the wire length was taken identical to the rod length and the length increase due to the helix was not taken into account. For the worst case (P/D = 1.1; H/D = 8.3) this results in an inaccuracy of < 0.6 % in U_B which was accepted. G depends very much on the number of rods, Z, and only very little on the P/D ratio:

$$\frac{1}{G} = 1 + \frac{(\sqrt{12\ Z - 3} - 3)\ \cos 30 + 6}{\cos 30\ \pi\ Z} - \frac{3}{(P/D)\ \cos 30\ \pi \cdot Z} \qquad (15)$$

$$Z = \infty \rightarrow \quad G = 1$$

The factor F takes into account the ratio of the flows in the bundle with spacer wires to the purely axial bundle flow.

$$\bar{u}'/\bar{u} = \sqrt{F} \qquad (16)$$

Therefore, it is dependent on the helical lead-to-rod diameter and the rod pitch-to-diameter ratios:

$$F = \sqrt{P/D} + (7{,}6 + (P/D)^3/(H/D)^{2.16} \qquad (17)$$

In the setup for this equation the flow is assumed to be forced around the rod by the helical wire. The exponent was derived from fitting the equation to the experimental results /1/. For the range of tight rod packings investigated, the blockage of subchannels by the helical wires recognizable in the projection area decreases in the direction of lower P/D ratios (Fig. 1), while the radial resistance increases as a consequence of the reduction in distance of the adjacent rods. As a result, Equation (17) is no longer applicable to this range. The agreement between experimental results and computed results was improved by setting up for the correction factor F a double polynomial in P/D and H/D, compared to Equation (17). The fitting function was set up for the range of 1200 < Re < 500,000, namely:

$$F = \sum_{j=1}^{3} \sum_{i=1}^{5} Q_{j,i}\ (P/D)^{i-1}\ (H/D)^{1-j} \qquad (18)$$

In the approximation to the measured data of this function the following constants Q were calculated:

i / j	1	2	3	4	5
1	- 35.86961	105.2234	-105.9738	42.95216	-5.279805
2	- 22145.98	74589.58	-93864.92	52318.52	-10900.42
3	127095.0	-440977.3	570743.0	-327052.1	70186.30

The pressure loss coefficients were calculated by means of Equation (18) for Re = 30,000 and represented in Fig. 15 as a function of P/D and H/D with the experimental results. Compared to Fig. 14, an improvement is seen in the agreement between the experimental results and computed results for low P/D ratios. The attempt to include in the determination of constants for Equation (18) the measured data for P/D = 1 was not pursued in the present state.

3.2.2 Laminar Flow

As also data measured in the regime of laminar bundle flow were determined, an approach to calculations was sought also in this flow range as this could not be found in the literature. The studies of laminar flow in rod bundles without spacers according to /12; 13/ were used for this purpose. The pressure loss consequently is calculated as follows:

$$\Delta p = K_o \, L \, \bar{u} \quad \eta/2d_h^2 \tag{19}$$

Substituting Equations (1) and (5) in (19) results in the pressure loss coefficient as:

$$\lambda = K_o/Re \tag{20}$$

Because of the conditions prevailing in a bundle geometry, the pressure loss in all subchannels is equal to the total pressure loss in the bundle. If this condition is taken into account, the geometry factor of the bundle is defined as follows:

$$1/K_o = \sum_{i=1}^{n} (1/K_{(i)})(U/U_{(i)})^2 (A_{(i)}/A)^3 \tag{21}$$

The specific geometry factors of the three channel types of a hexagonal rod bundle show the following dependencies:

Central channel:	$K_{(i)} = f(P/D)$.
Wall channel:	$K_{(i)} = f(P/D;\ W/D)$.
Corner channel:	$K_{(i)} = f(W/D)$.

These dependencies were determined experimentally in /12/ and apply only to bundles without spacers.

In the bundles with wire spacers for equal P/D ratios, the channel geometries, i.e., the cross section and the wetted perimeter of the channels, change. For this reason, an attempt was made to convert the specific geometry factors of the channel types by means of the hydraulic diameter of the channel (Equation 2). As the axial blockages of the subchannels by the wires are small for the tightly packed rod bundles investigated, and the bundle flow therefore more closely approximates a purely axial main flow, that approach can be defended.

Equation (19) was used for conversion. In this way, the geometry factors specific to channels of bundles with spacers are calculated as follows:

$$K_{(i)}^{*} = K_{(i)} \left(d_{h(i)}^{*}/d_{h(i)}\right)^2 \qquad (22)$$

The asterisk characterizes the data for bundles with spacers, those data determined according to /12/ are without asterisk.

$$\sqrt{F}/K_o = \sum_{i=1}^{n} (1/K_{(i)}^{*})(U^{*}/U_{(i)}^{*})^2 \left(A_{(i)}^{*}/A^{*}\right)^3 \qquad (23)$$

Considering the correction factor in Equation (23) for the flow behavior within the bundles with helical wire spacers results in the geometry factors $K_{o(R)}$ for the different P/D and H/D ratios. These computed magnitudes $K_{o(R)}$ are compared with those evaluated from the experiments $K_{o(E)}$ by means of the least squares of deviations in the following table:

	Calculation ($K_{o(R)}$)			Experiment ($K_{o(E)}$)			Deviation $K_{o(R)}/K_{o(E)}$		
H/D / P/D	8.3	12.5	16.7	8.3	12.5	16.7	8.3	12.5	16.7
1.022	36.7	36.2	35.9	33.5	35	34.9	1.10	1.03	1.03
1.041	53.9	50.3	48.7	46.6	42.9	46.3	1.16	1.17	1.05
1.072	75.8	66.8	63.0	68.7	57.0	56.8	1.10	1.17	1.10
1.101	92.6	78.7	72.4	82.3	74.5	69.3	1.13	1.06	1.04

The deviations $K_{o(R)}/K_{o(E)}$ reveal that the calculated values are 9.5 % higher than those gained from the experiments as an average.

The pressure losses are calculated using Equation (19) under consideration of the modified K_o value according to Equation (23).

Equation (21) takes into account the number of rods in the bundle, which is why, in contrast to the pressure loss coefficients for turbulent flow, the correction factor, G, is not included.

3.2.3 Range of Application

The limits of application of these correlations are defined as follows on the basis of experimental findings:

o Laminar flow regime:

$$50 < Re\sqrt{F} < 65/((P/D)-1)^{0.712}$$
$$1.02 < P/D < 1.10$$
$$8.3 < H/D < 16.7$$

o Turbulent transition regime:

- Tight rod packing:

$$91((P/D)-1)^{0.712} < Re\sqrt{F} < 19{,}000$$
$$1.02 < P/D < 1.10$$
$$8.3 < H/D < 16.7$$

- Wide rod packing:

$$2000 < Re\sqrt{F} < 19{,}000$$
$$1.13 > P/D < 1.42$$
$$8.3 < H/D < 50$$

o Fully turbulent flow regime:

- Tight rod packing:	$19{,}000 < Re\ \sqrt{F} < 100{,}000$
	$1.02 < P/D < 1.10$
	$8.3 < H/D < 16.7$
- Wide rod packing:	$19{,}000 < Re\ \sqrt{F} < 500{,}000$
	$1.13 < P/D < 1.42$
	$8.3 < H/D < 50$

4. PRESENTATION OF COMPUTED AND MEASURED PRESSURE LOSS COEFFICIENTS

To demonstrate the degree of approximation of computation and the own experiments the results are shown in different diagrams. Fig. 15 only applies to one measurement each in a series of measurements for a bundle exposed to a fully turbulent bundle flow at Re = 30,000. The measured and the calculated data were plotted as a function of the Reynolds number for the twelve bundles in Figs. 16-19. The measured data were represented with differing symbols, the computed data as a scatter band with the following bandwidths for the different flow regimes:

Laminar flow regime:	$\pm$ 10 %.
Turbulent transition regime:	$\pm$ 10 %.
Fully turbulent flow regime:	$\pm$ 5 %.

The diagrams show the mean error, the variance, the root mean square, and the number of computed and measured points. The diagrams reveal the following findings:

- The differences between calculations and measurements are a minimum in the fully turbulent flow regime and a maximum in the laminar flow regime.
- Only very few measured points are outside the given bandwidths of calculation.

Summarizing it can be stated that the computation method in hand represents the experimental data for practical applications with an adequate accuracy.

5. COMPARISON OF MEASURED DATA FROM THE LITERATURE AND COMPUTED DATA

5.1 Bundles with helical wires

A large number of measured pressure loss coefficients exists for various P/D and H/D ratios as well as rod numbers. Most of the data had to be extracted from diagrams for this comparison. As in most cases geometrical tolerances of the used test sections are not reported ideal geometrical conditions were assumed for the recalculations. This is unavoidably associated with inaccuracies which should be taken into account in the comparison. The computations were based on a scatterbund with $\pm$ 5 % for the fully turbulent regime and $\pm$ 10 % for the turbulent transition and laminar regimes. In addition to the characterstic data of the bundles, the mean difference, the standard deviation and the root mean square are indicated.

For 14 rod bundles with the following characteristic data, pressure loss coefficients as a function of the Reynolds number were published by T.C. Reihman /14/:

P/D	1.06	1.06	1.12	1.12	1.12	1.12	1.12	1.12	1.12	1.12	1.17	1.18	1.32	1.32
H/D	22.6	45.1	12	24	48	40	48	48	61.2	96	50	50.9	24	48
Z	37	37	37	37	37	37	19	217	37	37	37	37	37	37
Fig.	20	20	21	21	21	22	23	23	22	22	24	25	26	26

In Figs. 20-26, the measured data are indicated as dots, the computed data as a scatterband. Most of the measured data are within the calculated bandwidths.

Pressure loss coefficients determined by C. Chiu et al. /15/ for two bundles with 61 rods of the same P/D ratio of 1.067 and various H/D ratios were transferred as diagrams into Figure 27 and compared with computed pressure loss coefficients. The diagrams indicate rather good agreement for the turbulent regimes. Only one measured point within the laminar flow regime for the bundle with a very small helical lead-to-diameter ratio of H/D = 4 differs greatly from the computed value.

The pressure loss coefficients for the bundle with 37 rods, a P/D ratio of 1.154, and a H/D ratio of 13.4 in Fig. 28 were made available to us as numerical data by S.K. Cheng. They had been published in /16/. Comparison with

the computed values shows good agreement also in this case. All pressure loss coefficients apply to the turbulent flow regime.

Pressure loss coefficients for a 127-rod bundle by G. Cornet /7/ were taken from the report as numerical data. The measured data for the bundle with P/D = 1.19 and H/D = 30, compared with the computed results in Fig. 29, again show good conformity.

Agreement with the computed data is found also in a comparison of the pressure loss coefficients measured by Hoffmann /2/ for the three bundles with P/D = 1.32 and H/D = 16.7, 33.3, 50 (Fig. 30).

Comparing computed and measured data communicated in /17/ and /18/ a very satisfying correspondence can be found for the bundles with rod numbers $Z > 19$ in the turbulent and laminar flow regimes, Fig. 31 and 32. The datas of Fig. 33 for a 19-rod bundle investigated in a sodium flow are still in a satisfying accordance to the computations.

5.2 Bundles with Finned Tubes

Unlike wire spacers wound helically on rods, also helical fins directly drawn on rod claddings can be used as spacers. Tubes with three and six fins have been made, and the pressure loss coefficients of bundles with finned tubes were included in the comparison. As is shown by the cross section of a central channel in a bundle with finned tubes, the height of the fins amounts to half the wire diameter at the same P/D ratio. In a finned tube of the same H/D ratio, depending on the number of fins, there are more blockages in the subchannels of the bundle. Hence, it is not to be taken for granted that the four bundles with 6- and 3-finned tubes in Figs. 34 to 36 showed good agreement between the measured and the computed pressure loss coefficients. All bundles have high P/D ratios of 1.32 /2/ and 1.17 /3/. In the bundle with 6-finned tubes, for a very low P/D ratio of 1.03 /17/, the calculated pressure loss coefficients are slightly higher than the measured ones, as is shown in Fig. 36. The very low fin heights of 0.25 mm hardly protrude from the laminar sublayer on the rods of 16.1 mm diameter. The diameters of the spacer wires would still be 0.5 mm by comparison.

6. SUMMARY AND CONCLUSION

Systematic measurements of the pressure loss coefficients performed on 37-rod bundles with wire spacers in tight rod packings were performed for the following parameters:

Re: $50 < Re < 90{,}000$.
P/D: 1.02; 1.04; 1.07; 1.10.
H/D: 8.3; 12.5; 16.7.

Because of the high precision achieved in fabrication of the bundles, and detailed investigations of the appropriate technical measurement methods it was possible to determine the pressure loss coefficients for the fully turbulent flow regime ($Re \sqrt{F} > 19{,}000$) with a maximum error of $\pm$ 5 % even for the lowest P/D ratio of 1.02. This error was doubled in the laminar flow regime.

The flow factor, F, was redetermined with these pressure loss coefficients for tight rod packings and with the data from /1/ for wide rod packings. The new flow factor together with the correlations from /1/ can be used to recalculate the pressure loss coefficients for bundles with tight and wide rod packings in turbulent flows.

An approach has also been shown to calculate pressure loss coefficients for tight rod packings and laminar bundle flows. Similar to the procedure for bare rod bundles /12/ a new geometry factor was evaluated based on these experiments.

The calculation method was applied to a multitude of data known from the literature on bundles with helical wire spacers and those with finned tube spacers for the turbulent and laminar flow regimes. As long as the bundle geometries are within the range of validity of the calculation method ($Z \geq 37$; $P/D \geq 1.02$; $H/D \geq 8.3$) a very good agreement between experiment and computation could be found.

7. NOMENCLATURE

A	flow cross section of bundle
$A_{(i)}$	flow cross section of subchannel
A_K	inner cross section of shroud
A_{St}	rod cross section
A_{Dr}	wire cross section
D	rod diameter
d	wire cross section
d_h	hydraulic diameter of bundle
$d_{h(i)}$	hydraulic diameter of subchannel
F	f(P/D, H/D) flow factor (Eq. 18)
G	f(Z; P/D) rod number factor (Eq. 15)
H	helical lead
K_o	geometry factor specific to a bundle (Eq. 21)
$K_{(i)}$	f(P/D; W/D) geometry factor specific to a channel (Eq. 22)
L	length
N	number of data in a series of measurements
P	rod pitch
Δp	pressure loss
Q	constants for Eq. 18
Re	Reynolds number (Eq. 5)
RMS	root mean square $(RMS)^2 = \sum_{i=1}^{n} X_{(i)}^2/(n-1)$
T	temperature
T_W	water temperature
U	wetted perimeter in bundle cross section
$U_{(i)}$	wetted perimeter in subchannel cross section
U_B	wetted perimeter of all rods and wires in bundle cross section
U_K	wetted perimeter of shroud in bundle cross section
u	local velocity
$\bar{u}$	mean velocity
u^+	dimensionsless velocity /8, page 556/
$\dot{V}$	volume flow
W	distance of rod from shroud wall plus rod diameter
$x_{(i)}$	percentage difference of specific data $x_{(i)} = ((\lambda_{M(i)}/\lambda_{R(i)})-1)\ 100$
$\bar{x}$	mean difference in series of measurements $\bar{x} = (1/n) \sum_{i=1}^{n} x_{(i)}$
y^+	dimensionsless wall distance /8, page 556/

Z	number of rods
ε	average peak-to-valley height of surfaces
λ	pressure loss coefficient
λ_M	pressure loss coefficient (measured)
λ_R	pressure loss coefficient (computed)
ν	kinematic viscosity of fluid
ρ	densitiy of fluid
σ	Standard deviation of measured data $\sigma^2 = (RMS)^2-(\bar{x})^2(n/n-1)$

8. LITERATURE

/1/ K. Rehme
Systematische experimentelle Untersuchung der Abhängigkeit des Druckverlustes von der geometrischen Anordnung für längs durchströmte Stabbündel mit Spiraldrahtabstandshaltern.
Dissertation TU Karlsruhe (1967)

/2/ H. Hoffmann
Experimentelle Untersuchungen zur Kühlmittelquervermischung und zum Druckabfall in Stabbündeln mit wendelförmigen Abstandshaltern.
KfK-1843 (1973)

/3/ H. Tschöke
Experimentelle Bestimmung des Druckverlustes an einem 37-Stabbündel aus Rohren mit 6 integralen Wendelrippen pro Stab als Abstandshalter.
KfK-1038 (Februar 1970)

/4/ K. Marten, S. Yonekawa, H. Hoffmann
Experimentelle Untersuchungen des Druckabfalles in eng gepackten Stabbündeln mit wendelförmigen Abstandshaltern.
KTG/DAtF Jahrestagung Kerntechnik, Mannheim 1982, pp. 133 - 136

/5/ K. Marten, S. Yonekawa, H. Hoffmann
Experimental Investigations on Pressure Drop in Tightly Packed Bundles with Wire Wrapped Rods.
2nd Internat. Specialists' Meeting on Thermal-Hydraulics in LMFBR Rod Bundles, Rome, I, September 15-17, 1982

/6/ K. Marten, J. Burbank, W. Hame, W. Hoffmann
Zusammenfassende Darstellung der Druckverlustbeiwerte von hexagonal angeordneten Stabbündeln mit Wendeldraht-Abstandshaltern für laminare und turbulente Strömungen.
KTG/DatF Jahrestagung Kerntechnik, Aachen 1986, pp. 54 -57

/7/ G. Cornet, G. Lamotte
Pressure Measurements in an SNR Mark-II Element with Spiral Wires.
BN 7707-02 (July 1977)

/8/ H. Schlichting
Grenzschichttheorie (1965), 5. Auflage, Verlag G. Braun, Karlsruhe

/9/ Yu. D. Levchenko, V.I. Subbotin, P.A. Ushakov, A.V. Sheynina
Geschwindigkeitsverteilung in der Zelle eines dicht gepackten Stabbündels. Liquid Metals, KfK-tr-371, pp. 223-234 (1967)

/10/ W. Eifler, E. Nijsing
Fundamental studies of fluid flow and heat transfer in fuel element geometries. EUR 2193e (1965)

/11/ W. Hame
LAMFIT, Programm zur Berechnung der Strömungsverluste. Bericht des Ingenieurbüros für Programmentwicklung in Thermo- und Fluiddynamik, Karlsruhe, unpublished report, (1983)

/12/ K. Rehme
Laminarströmung in Stabbündeln. Chemie-Ing-Technik 43, pp. 962-966 (1971)

/13/ K. Rehme
Laminarströmung in Stabbündeln. Reaktortagung des DAtF, Bonn, pp. 130-133 (1971)

/14/ T.C. Reihman
An Experimental Study of Pressure Drop in Wire-Wrapped FFTF Fuel Assemblies. BNWL-1207, Sept. 1969

/15/ C. Chiu et al.
Pressure Drop Measurements in LMFBR Wire-Wrapped Blanket Bundles.
Trans. ANS, Vol. 22 pp. 541-543 (1979)

/16/ S.-K. Cheng and N.E. Todreas
Fluid Mixing Studies in a Hexagonal 37 Pin Wire-Wrapped Rod Bundle.
MIT-Report, DOE/ET/37240-96TR, Febr. 82

/17/ Satoh, K., PNC, private Communication (1985)

/18/ Okada, T., PNC, private Communication (1985)

/19/ S. Yonekawa
Unpublished report of KfK, (1981)

Shroud:	Width across flats	SW = 103.05 ± 0.03 mm
	Distance of measurement planes	L = 125.0 ± 0.1 mm
Bundle rods:	diameter	D_1 = 16.21 - 0.011 mm
		D_2 = 16.87 - 0.011 mm
		D_3 = 15.35 - 0.011 mm
		D_4 = 14.87 - 0.011 mm
	mean surface roughness:	$\varepsilon \leq 0.3$ µm
Spacer wires:	diameter	d_1 = 0.35 ± 0.01 mm
		d_2 = 0.65 ± 0.01 mm
		d_3 = 1.10 ± 0.01 mm
		d_4 = 1.50 ± 0.01 mm

Table 1: Dimensions, tolerances, surface qualities of shrouds, rods and wire spacers.

Pressure Loss coefficient:	$\Delta\lambda / \lambda$	= ± 0.052
Reynolds numbers:	Δ Re/Re	= ± 0.016
Flow area:	Δ A/A	= ± 0.010
Wetted perimeter:	Δ U/U	= ± 0.001
Distance of measurement planes:	Δ L/L	= ± 0.001
Differential pressure:	$\Delta(\Delta p)/\Delta p$	= ± 0.005
Volume flow:	$\Delta \dot{V}/\dot{V}$	= ± 0.005
Fluid density:	$\Delta \rho / \rho$	= ± 0.005
Fluid viscosity:	$\Delta \nu / \nu$	= ± 0.01

Table 2: Maximum possible errors.

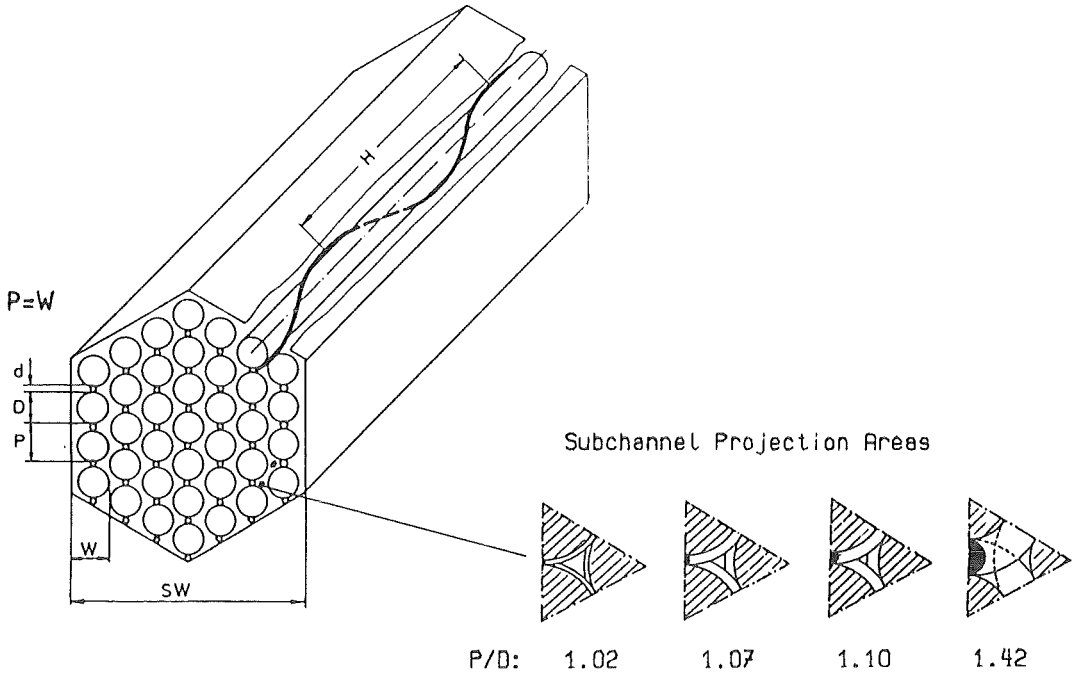

FIG.1 BUNDLE WITH HELICAL WIRE SPACERS

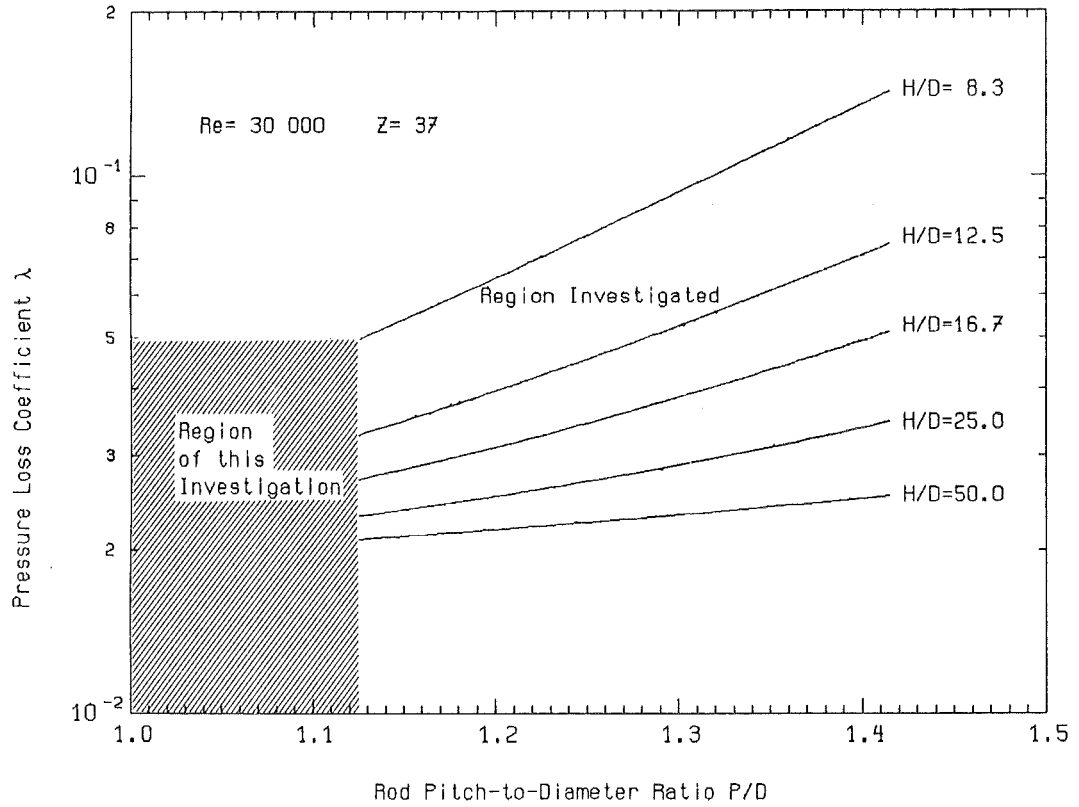

FIG.2 PRESSURE LOSS COEFFICIENT VS. THE P/D RATIO FOR DIFFERENT H/D RATIOS

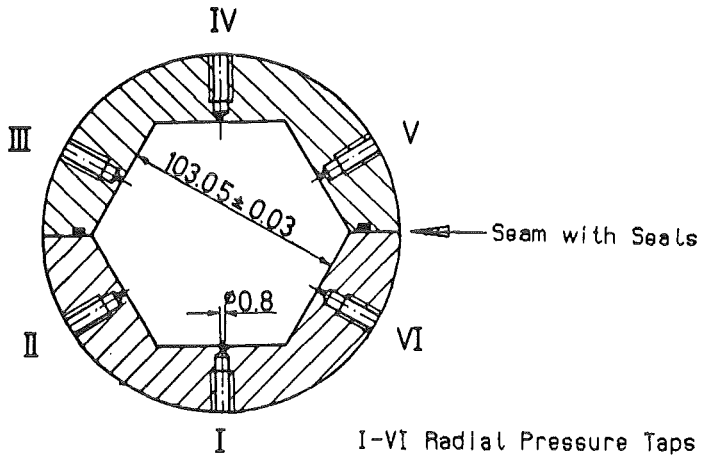

FIG.3 SHROUD OF THE BUNDLE

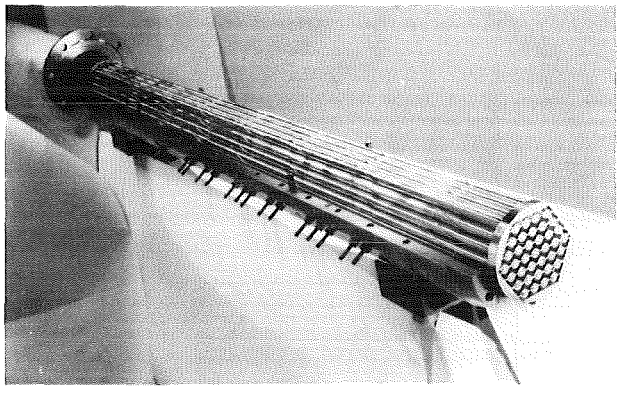

FIG.4 ASSEMBLED BUNDLE INSTALLED IN THE LOWER HALF OF THE SHROUD

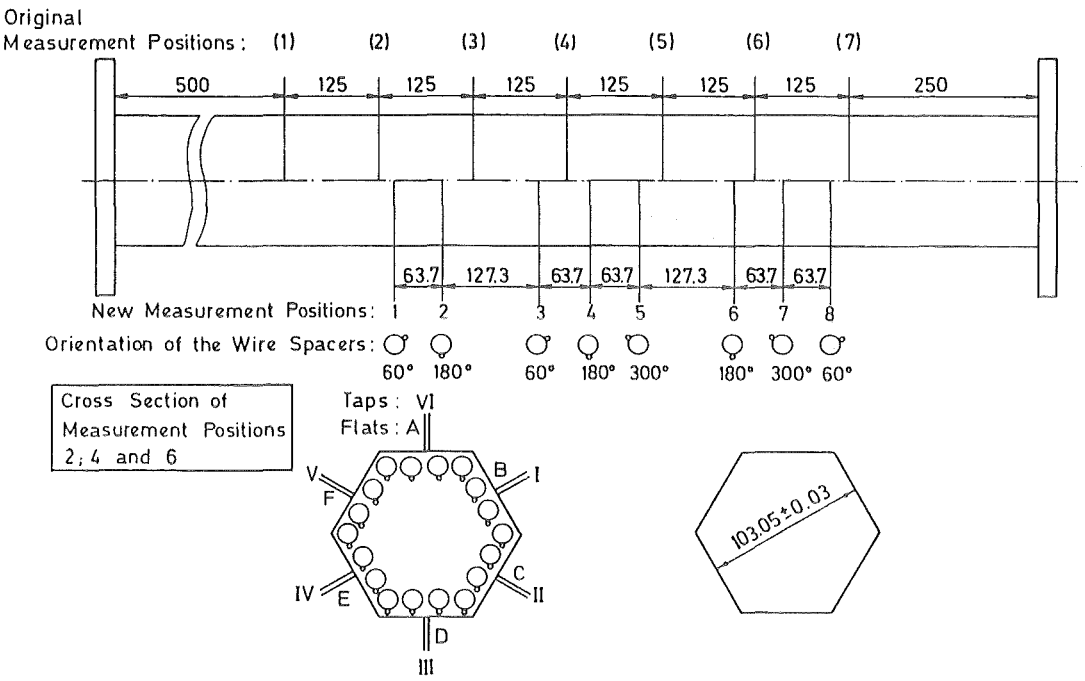

a) Arrangement of Pressure Messurement Taps and Orientations of the Wire Spacers on the Shroud

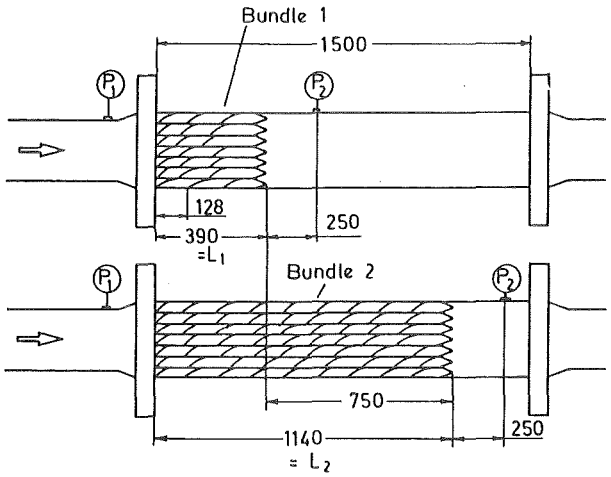

P_1 : inlet pressure measurement tap

P_2 : outlet pressure measurement tap

$$(\Delta P_{L1} - \Delta P_{L2}) = \lambda \frac{(L_1 - L_2)}{D} \frac{\rho U^2}{2}$$

b) Pressure Drop Measurement by Two Bundles of Different Lengths

FIG.5 PRESSURE DROP MEASUREMENT METHODS

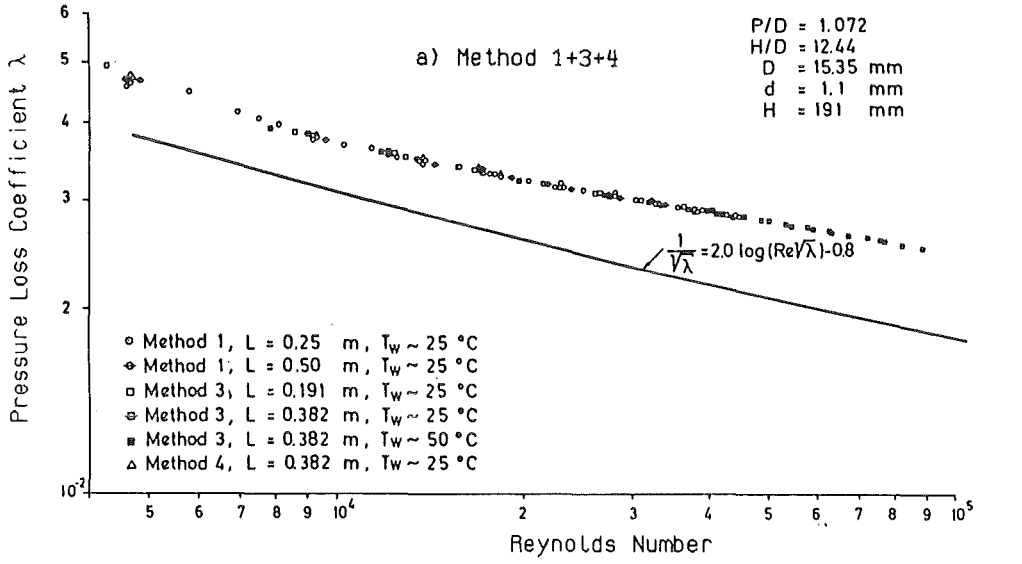

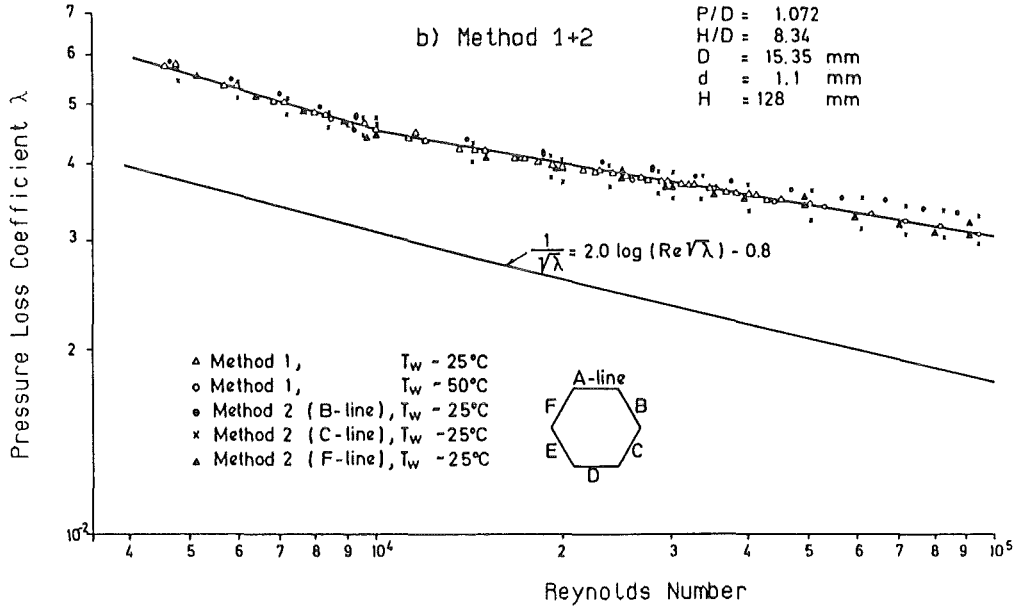

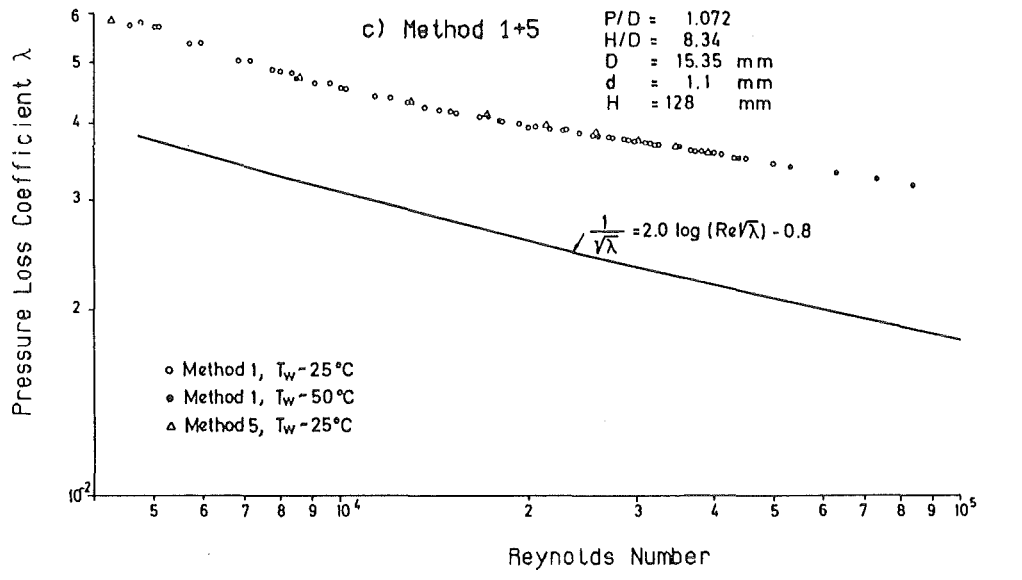

FIG. 6 PRESSURE LOSS COEFFICIENT AS A FUNCTION OF THE REYNOLDS NUMBER

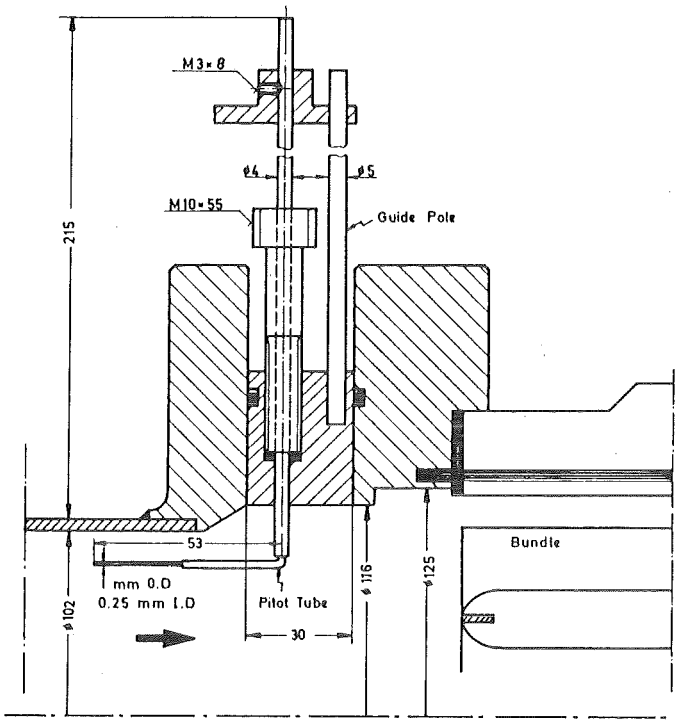

Measuring Devise with Movable Pitot Tube

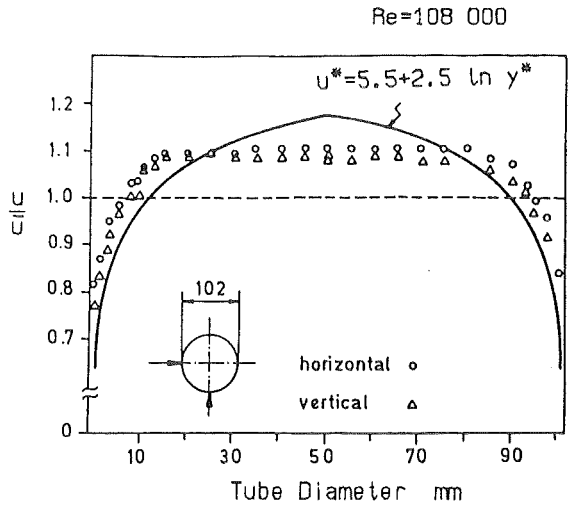

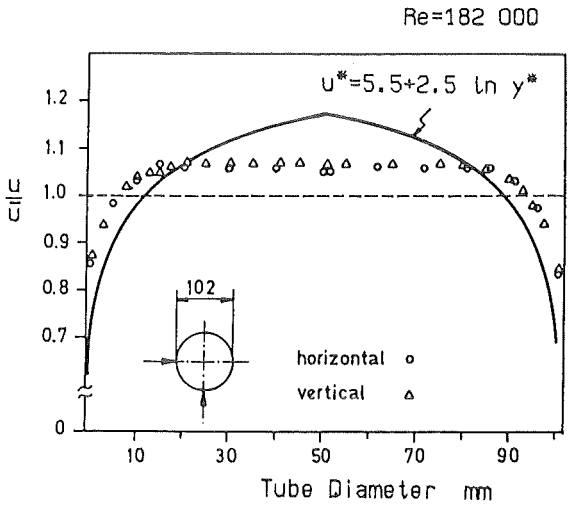

FIG.7 VELOCITY PROFILE AT THE INLET OF THE TEST SECTION

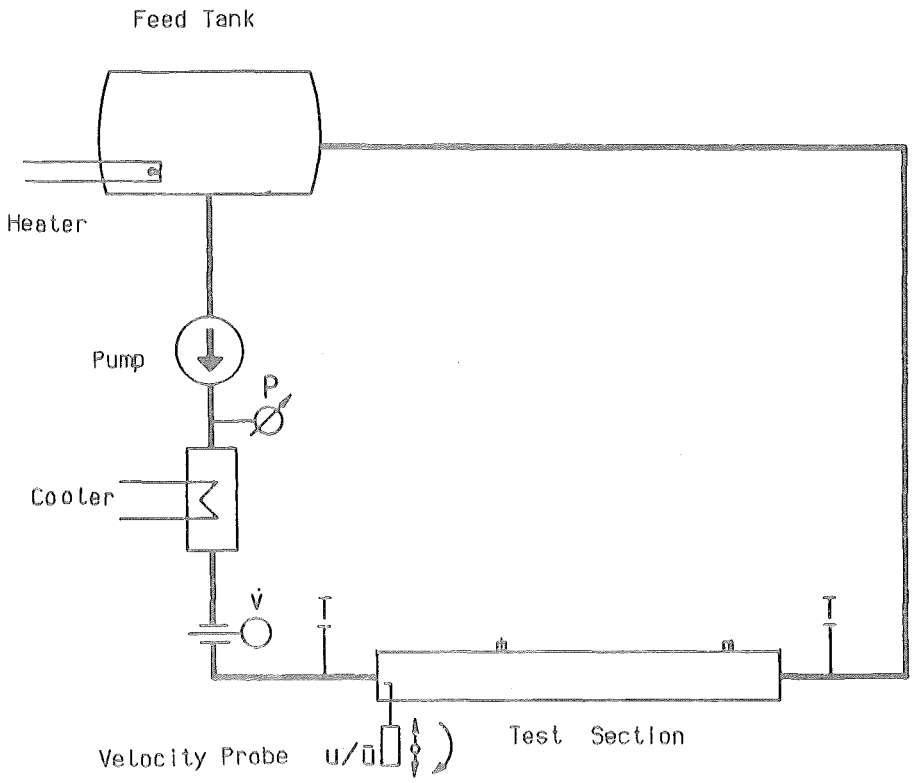

FIG.8 WATER LOOP

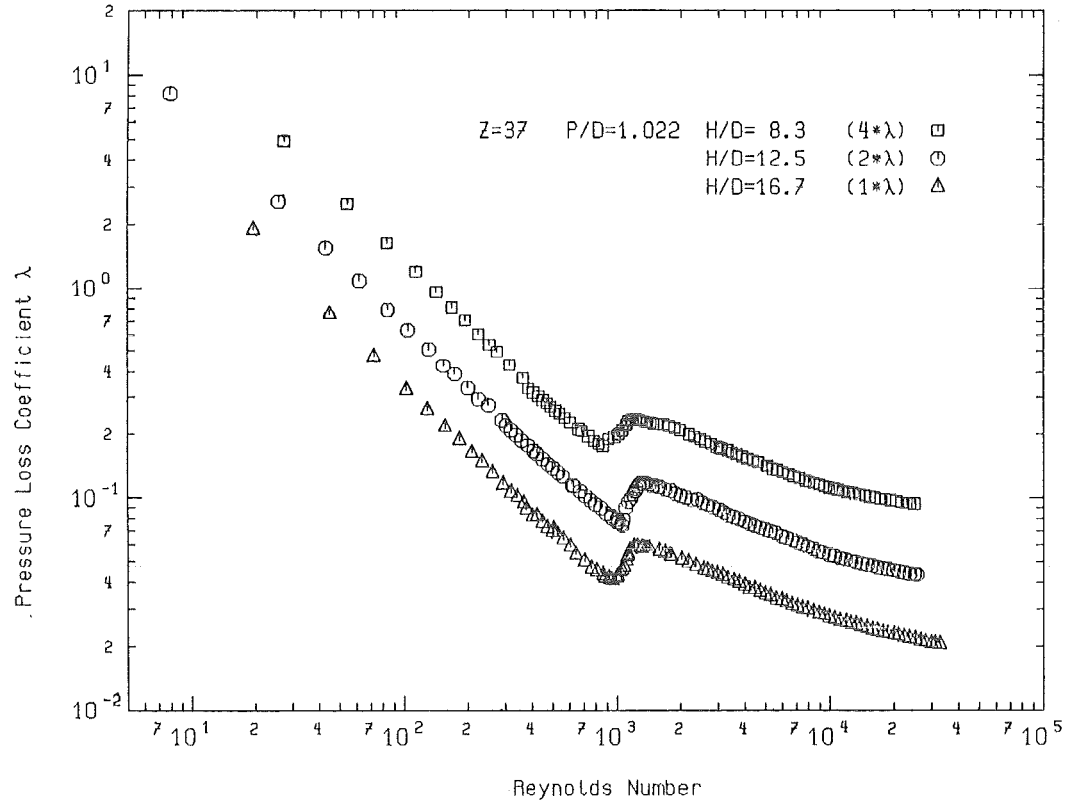

FIG.9 PRESSURE LOSS COEFFICIENT AS A FUNCTION OF THE REYNOLDS NUMBER

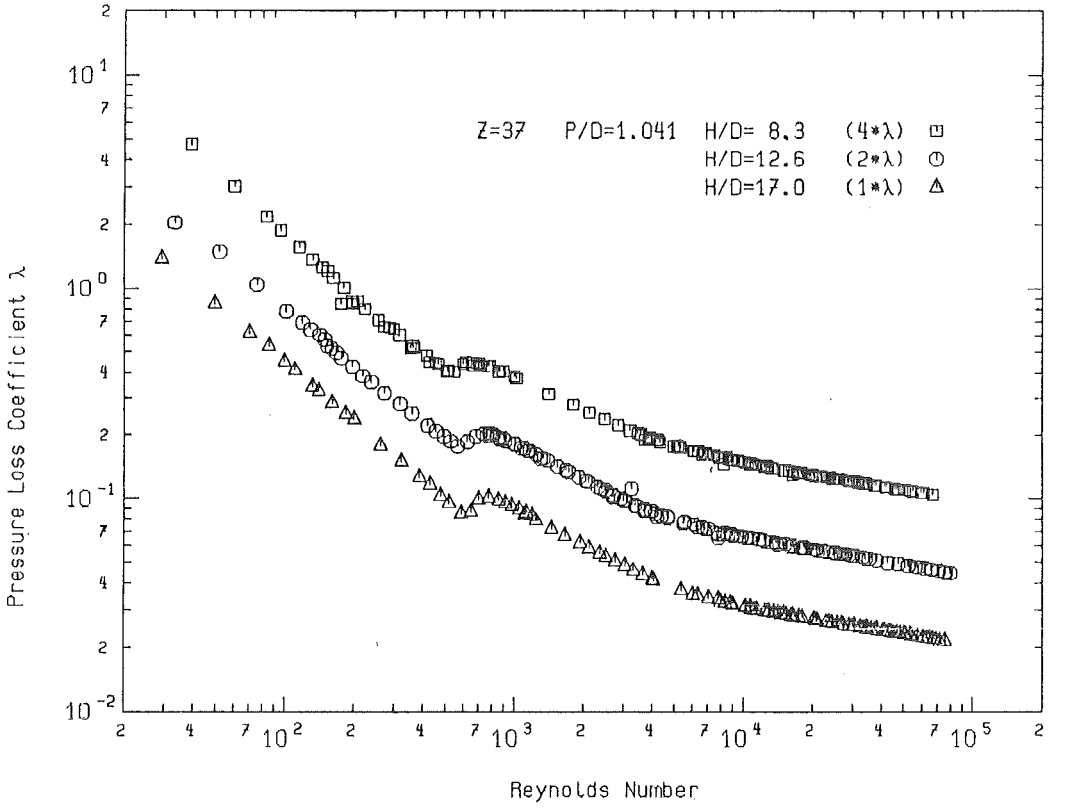

FIG.10 PRESSURE LOSS COEFFICIENT AS A FUNCTION OF THE REYNOLDS NUMBER

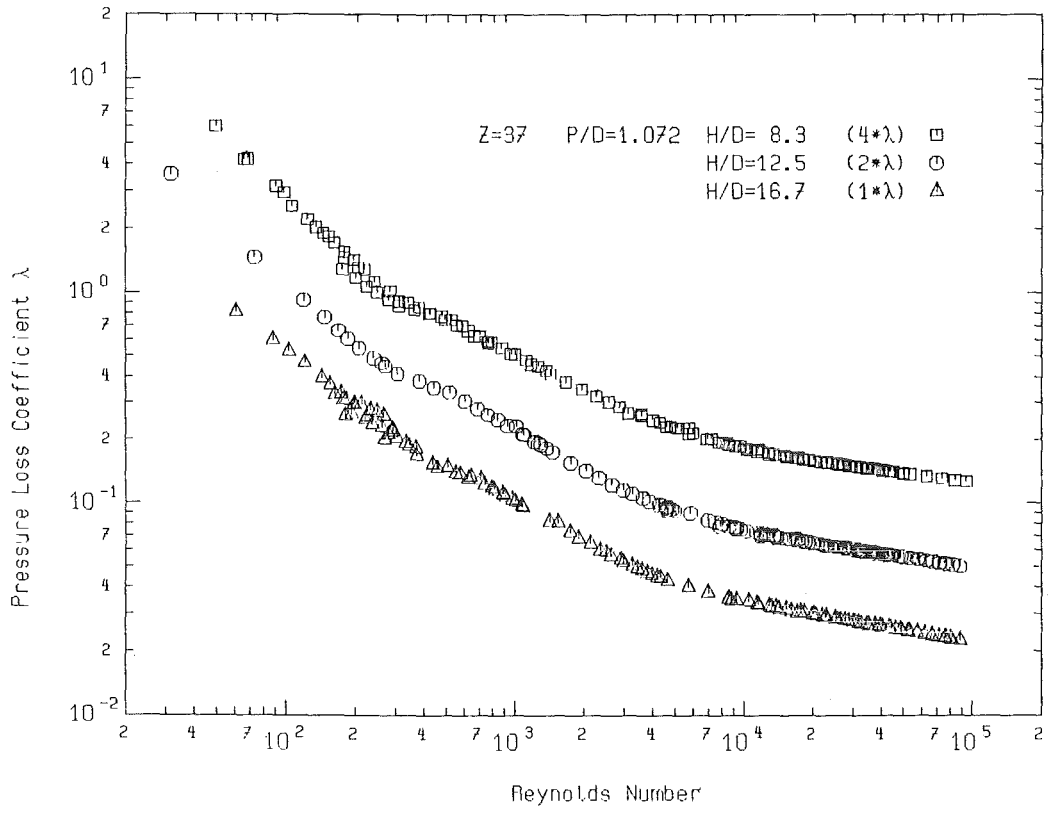

FIG.11 PRESSURE LOSS COEFFICIENT AS A FUNCTION OF THE REYNOLDS NUMBER

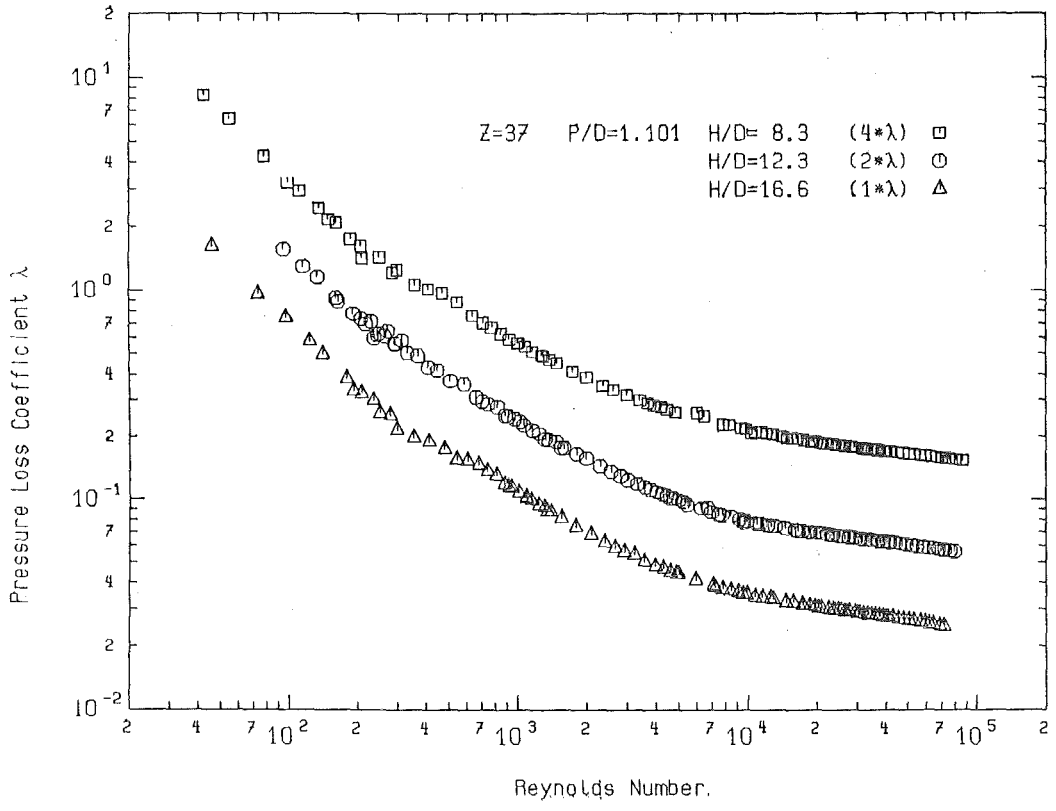

FIG.12 PRESSURE LOSS COEFFICIENT AS A FUNCTION OF THE REYNOLDS NUMBER

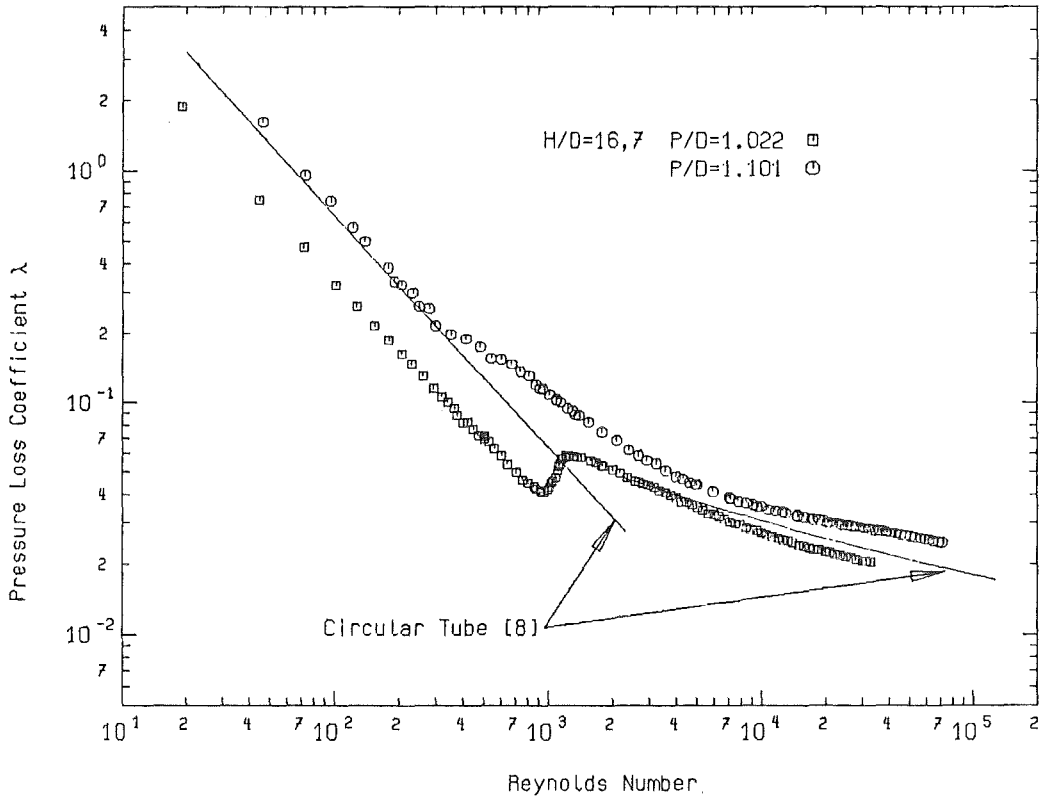

FIG.13 PRESSURE LOSS COEFFICIENT AS A FUNCTION OF THE REYNOLDS NUMBER

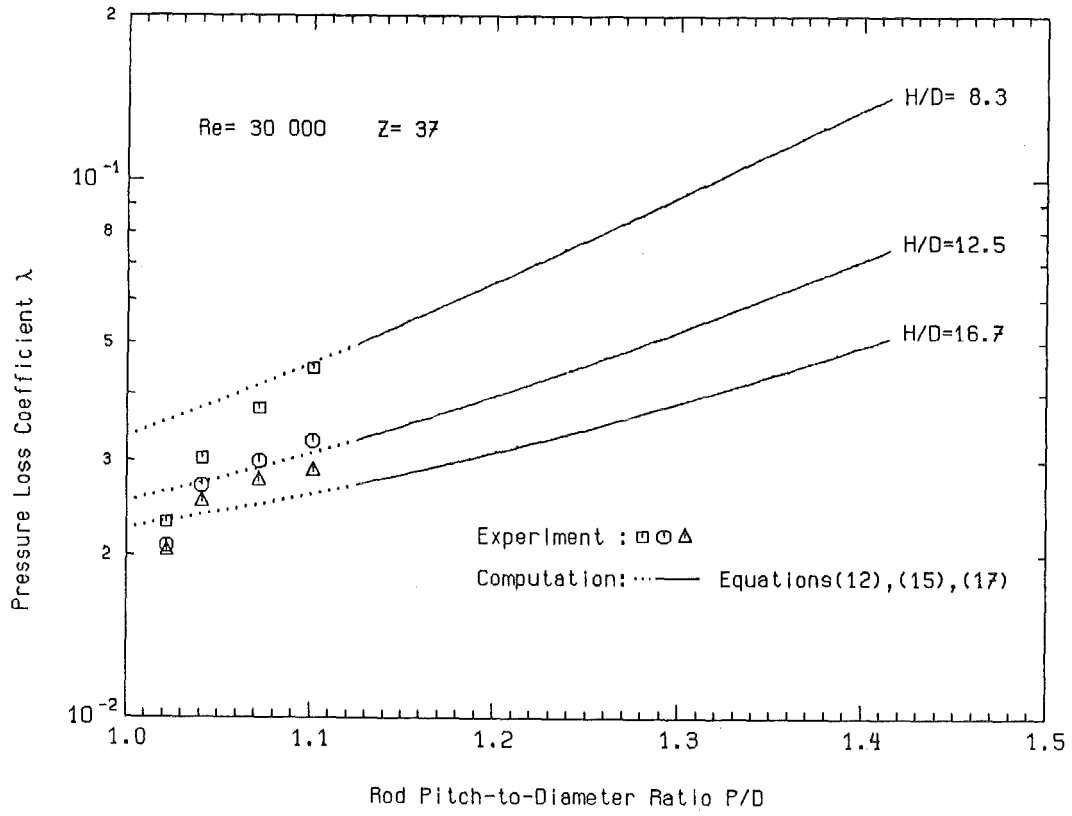

FIG.14 PRESSURE LOSS COEFFICIENT VS. THE P/D RATIO FOR DIFFERENT H/D RATIOS EXPERIMENT AND COMPUTATION

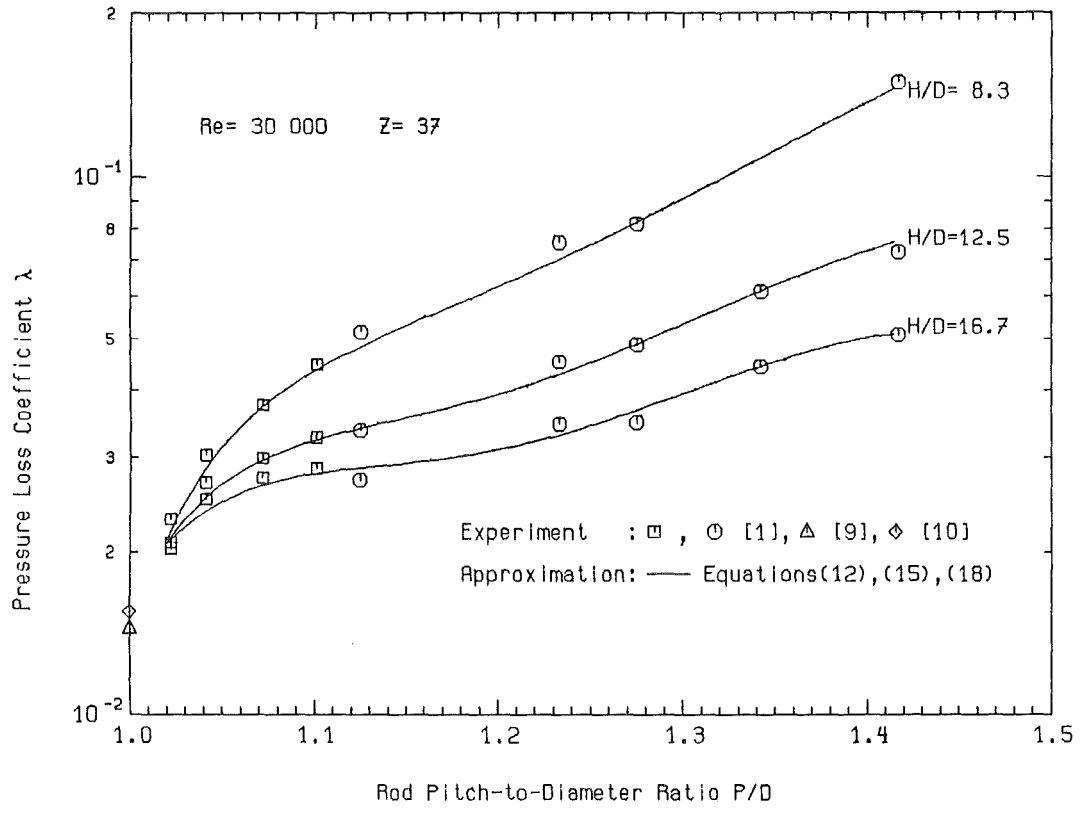

FIG.15 PRESSURE LOSS COEFFICIENT VS. THE P/D RATIO FOR DIFFERENT H/D RATIOS EXPERIMENT AND APPROXIMATION

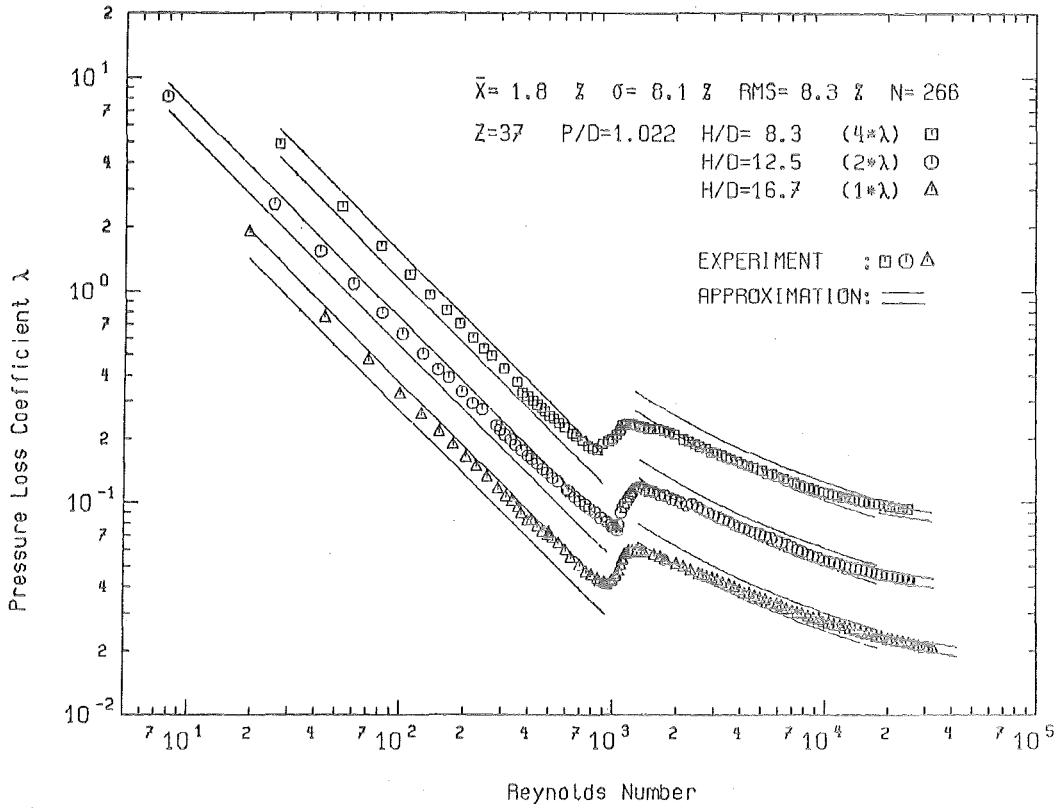

FIG.16 PRESSURE LOSS COEFFICIENT AS A FUNCTION OF THE REYNOLDS NUMBER
EXPERIMENT AND APPROXIMATION

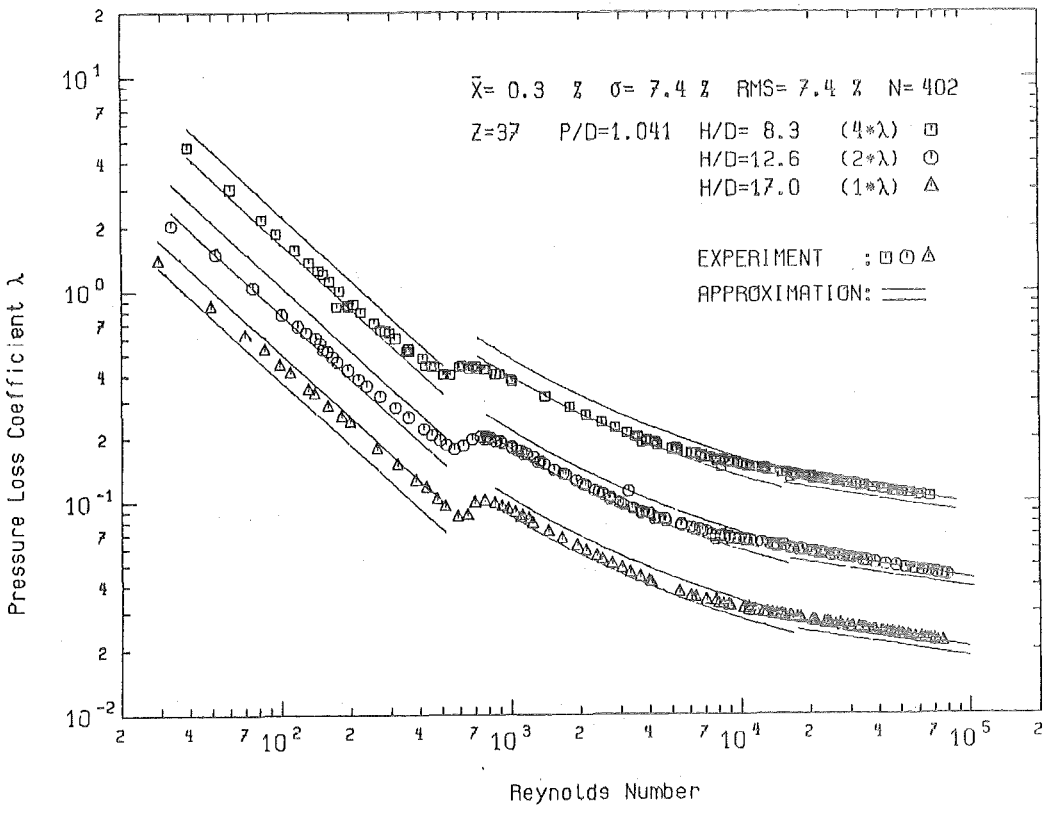

FIG.17 PRESSURE LOSS COEFFICIENT AS A FUNCTION OF THE REYNOLDS NUMBER
EXPERIMENT AND APPROXIMATION

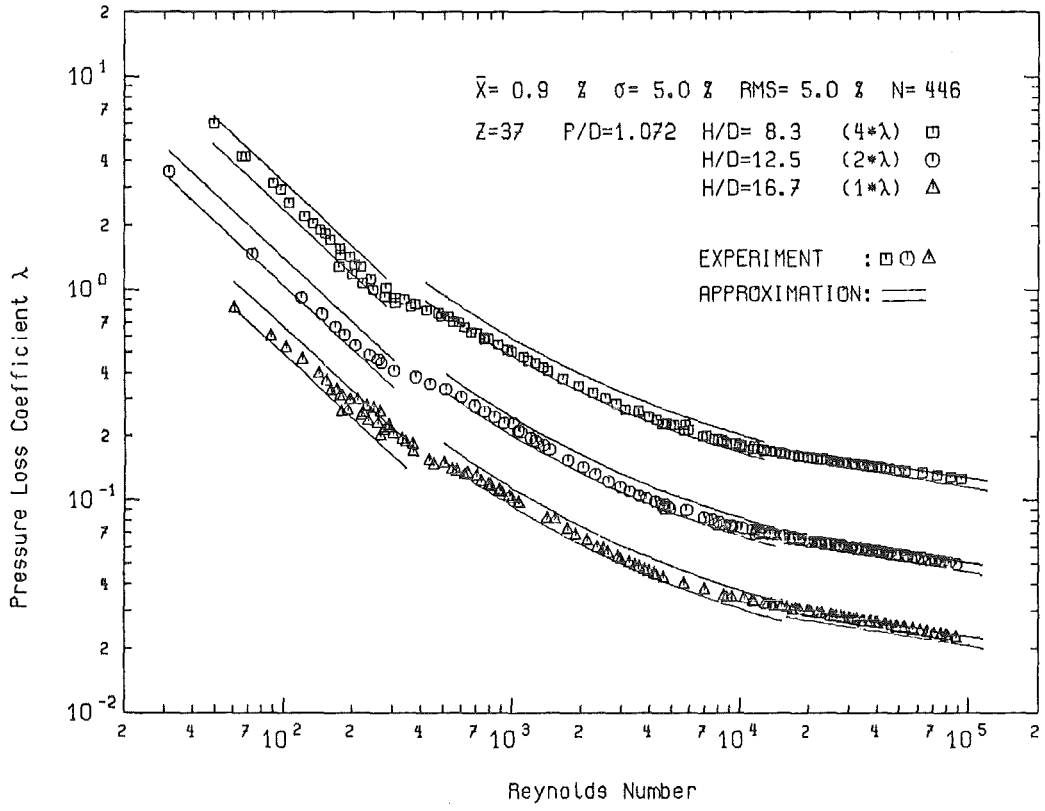

FIG.18 PRESSURE LOSS COEFFICIENT AS A FUNCTION OF THE REYNOLDS NUMBER EXPERIMENT AND APPROXIMATION

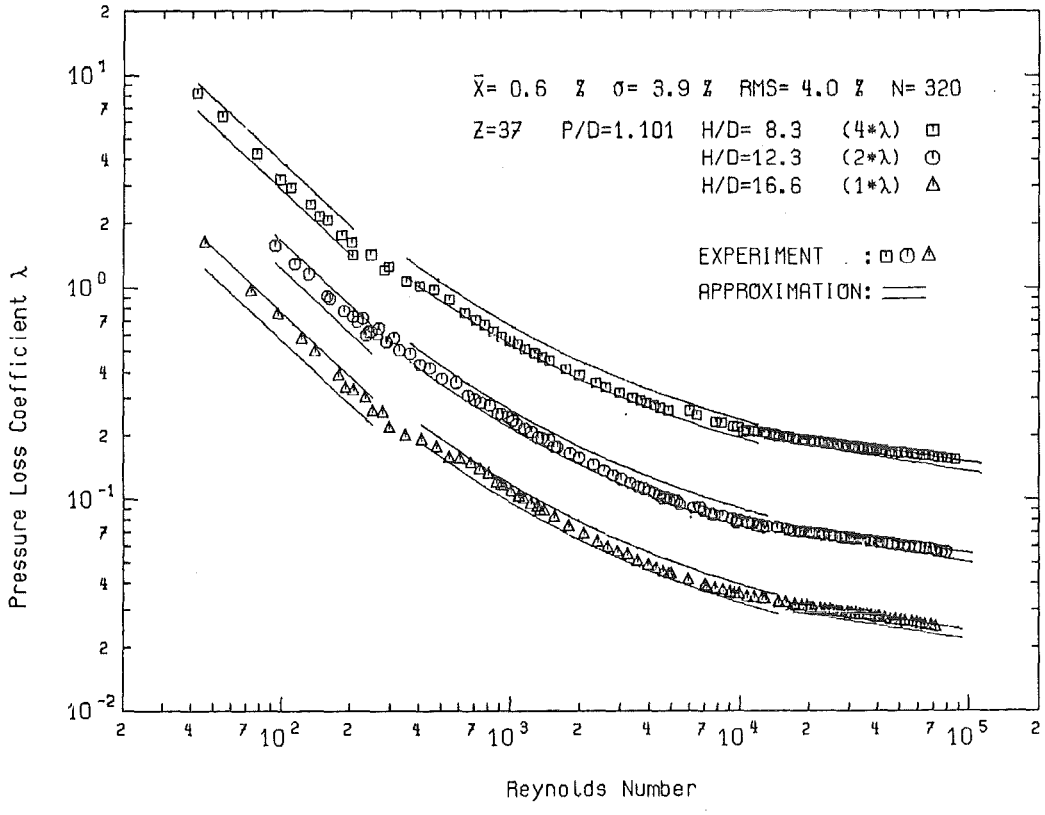

FIG.19 PRESSURE LOSS COEFFICIENT AS A FUNCTION OF THE REYNOLDS NUMBER EXPERIMENT AND APPROXIMATION

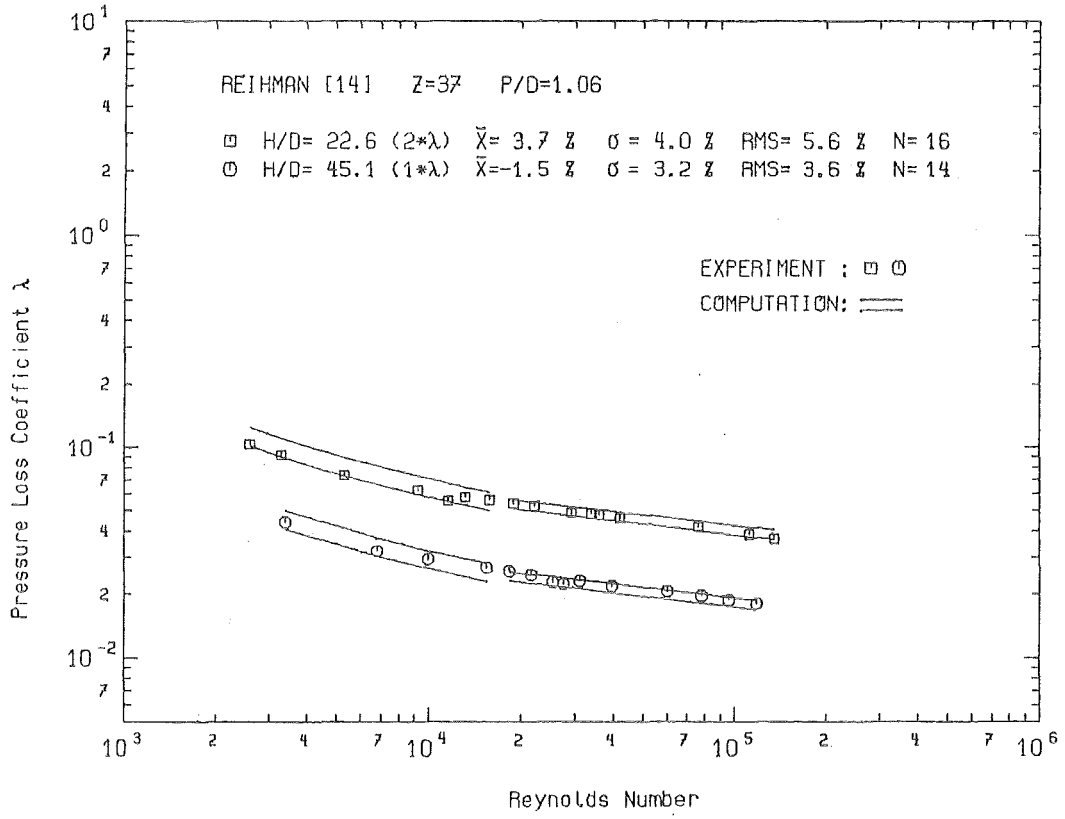

FIG.20 PRESSURE LOSS COEFFICIENT AS A FUNCTION OF THE REYNOLDS NUMBER EXPERIMENT AND COMPUTATION

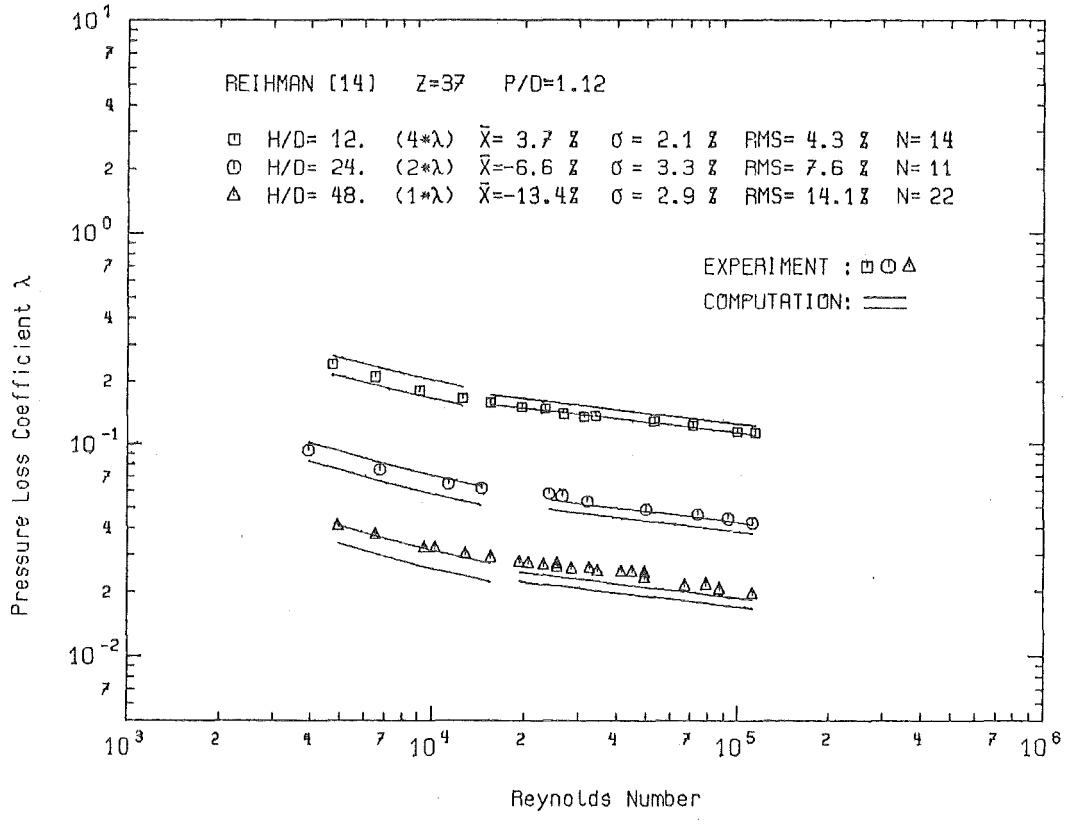

FIG.21 PRESSURE LOSS COEFFICIENT AS A FUNCTION OF THE REYNOLDS NUMBER EXPERIMENT AND COMPUTATION

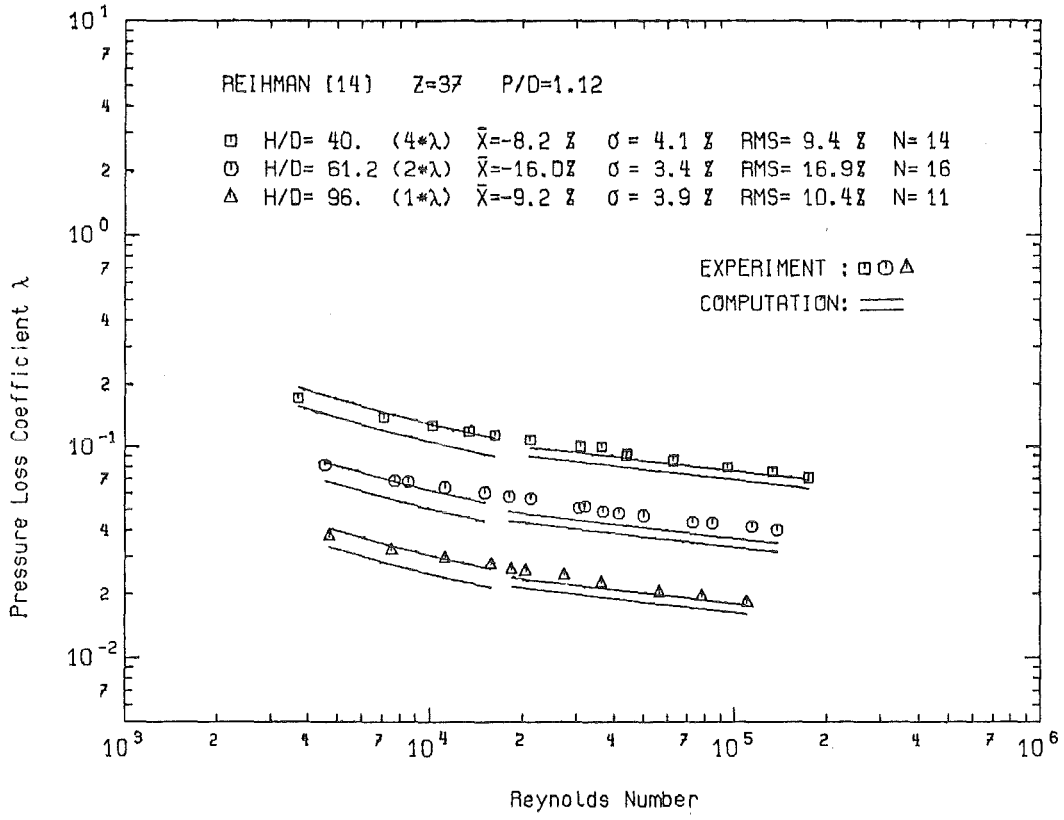

FIG.22 PRESSURE LOSS COEFFICIENT AS A FUNCTION OF THE REYNOLDS NUMBER EXPERIMENT AND COMPUTATION

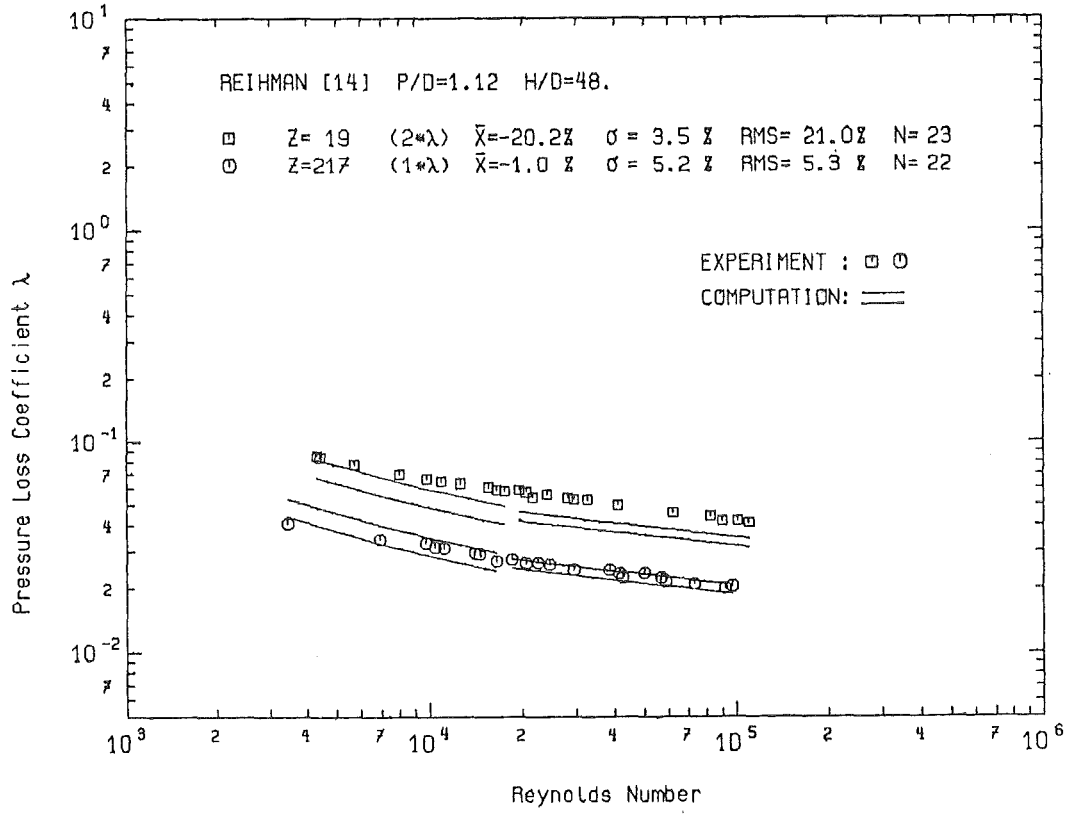

FIG.23 PRESSURE LOSS COEFFICIENT AS A FUNCTION OF THE REYNOLDS NUMBER EXPERIMENT AND COMPUTATION

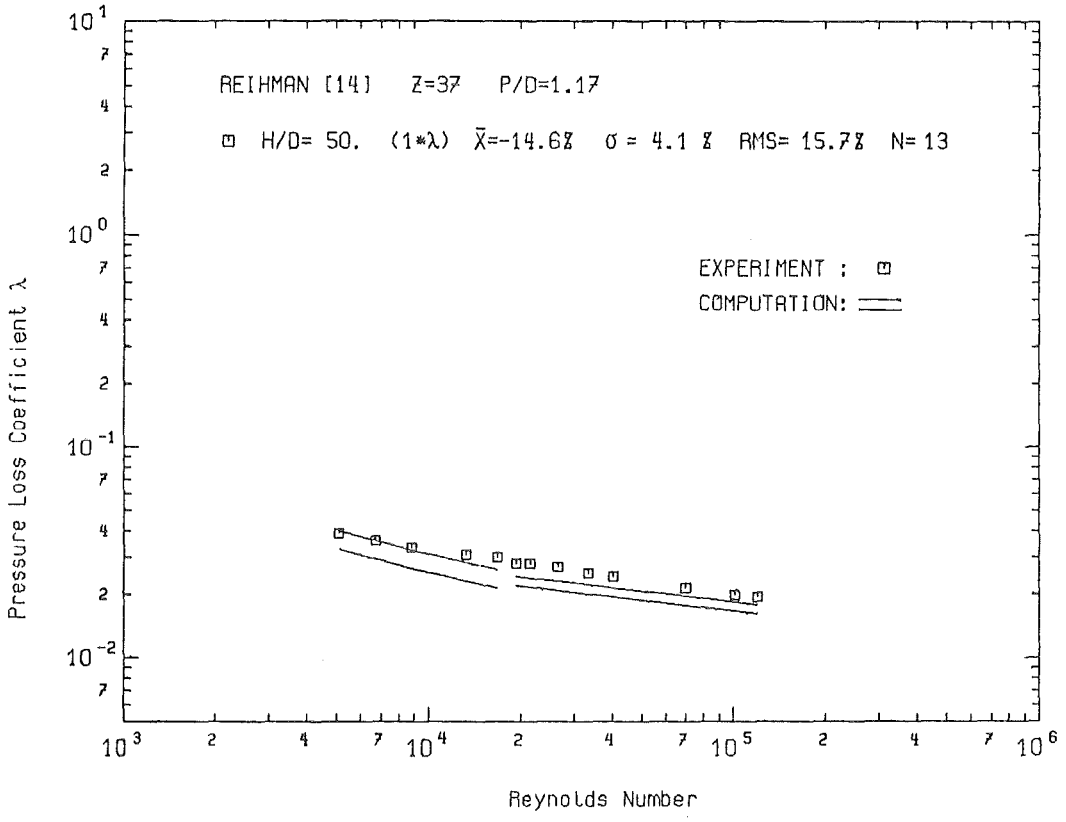

FIG.24 PRESSURE LOSS COEFFICIENT AS A FUNCTION OF THE REYNOLDS NUMBER EXPERIMENT AND COMPUTATION

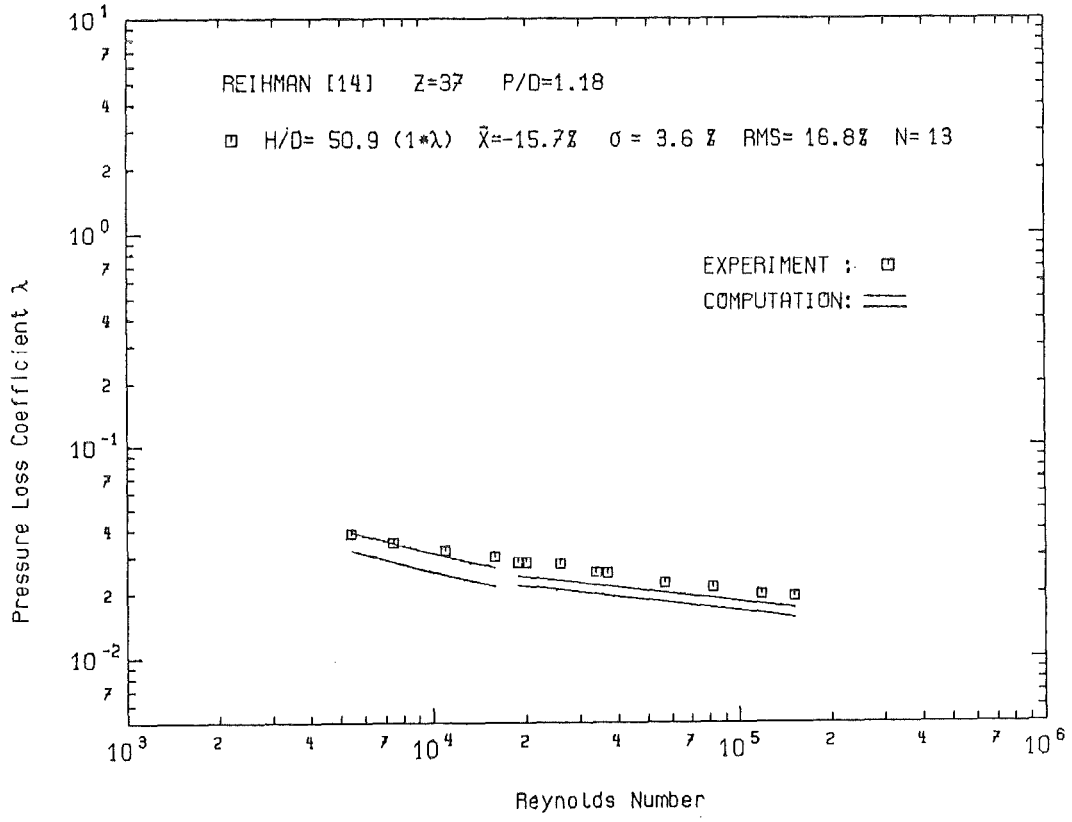

FIG.25 PRESSURE LOSS COEFFICIENT AS A FUNCTION OF THE REYNOLDS NUMBER EXPERIMENT AND COMPUTATION

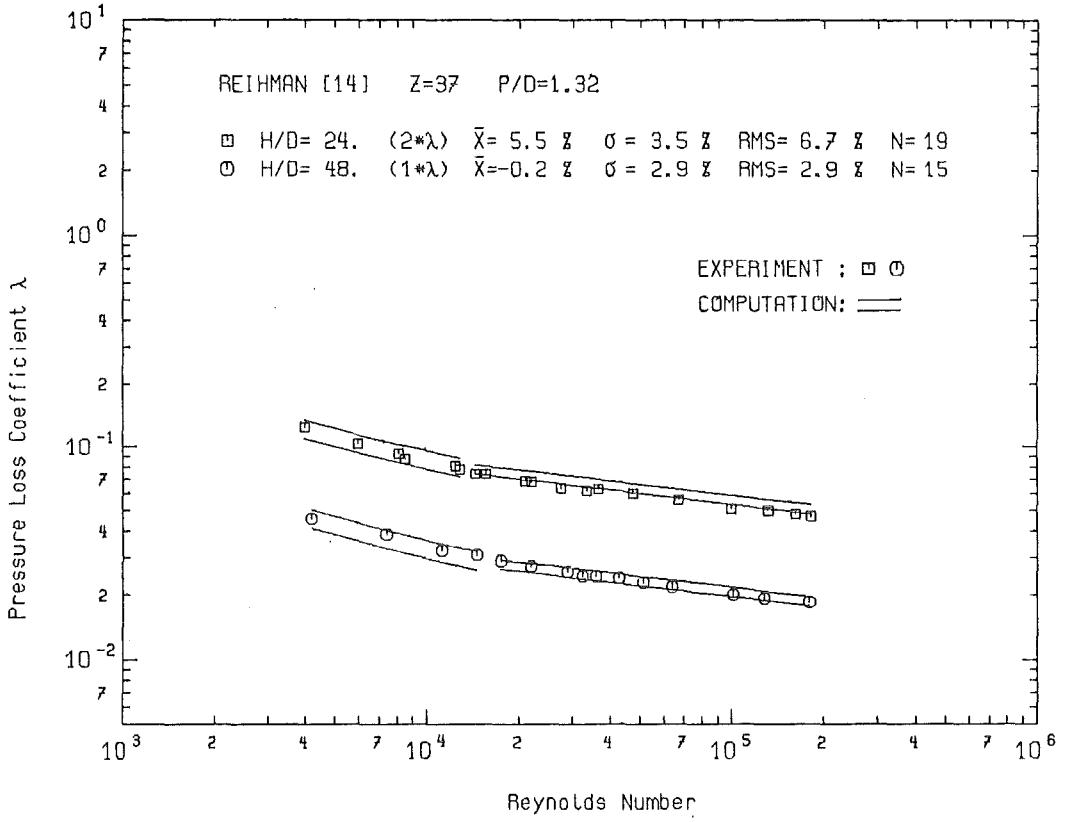

FIG.26 PRESSURE LOSS COEFFICIENT AS A FUNCTION OF THE REYNOLDS NUMBER EXPERIMENT AND COMPUTATION

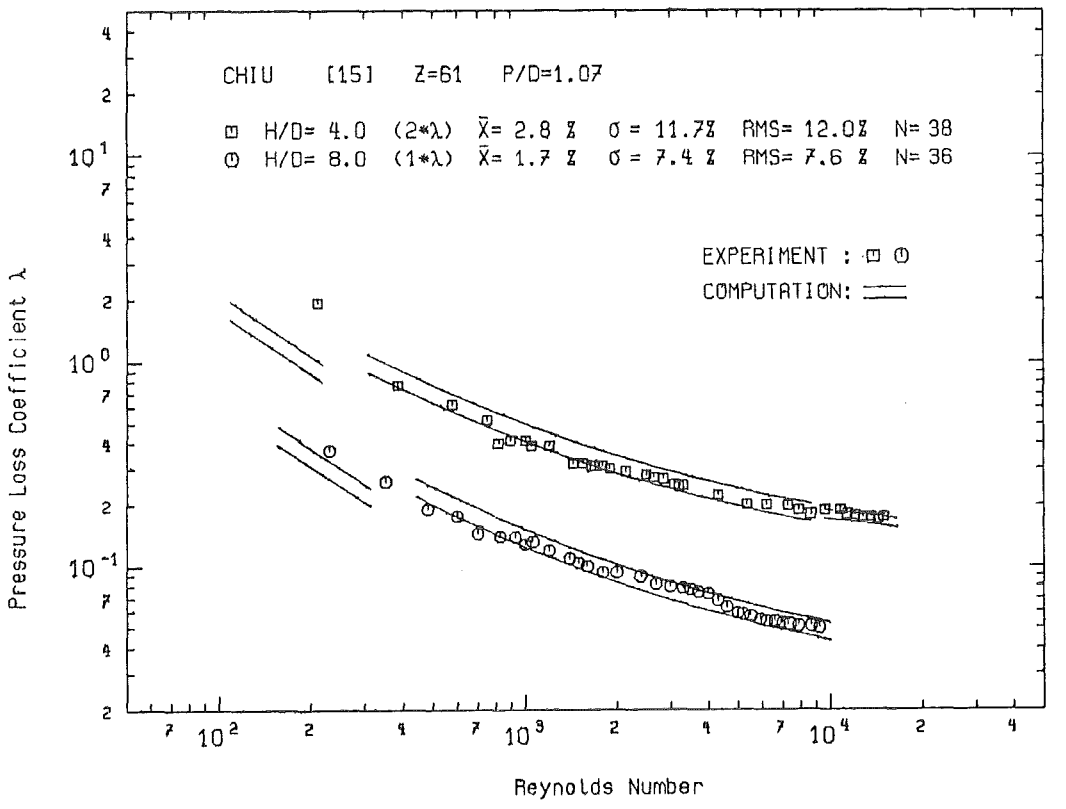

FIG.27 PRESSURE LOSS COEFFICIENT AS A FUNCTION OF THE REYNOLDS NUMBER EXPERIMENT AND COMPUTATION

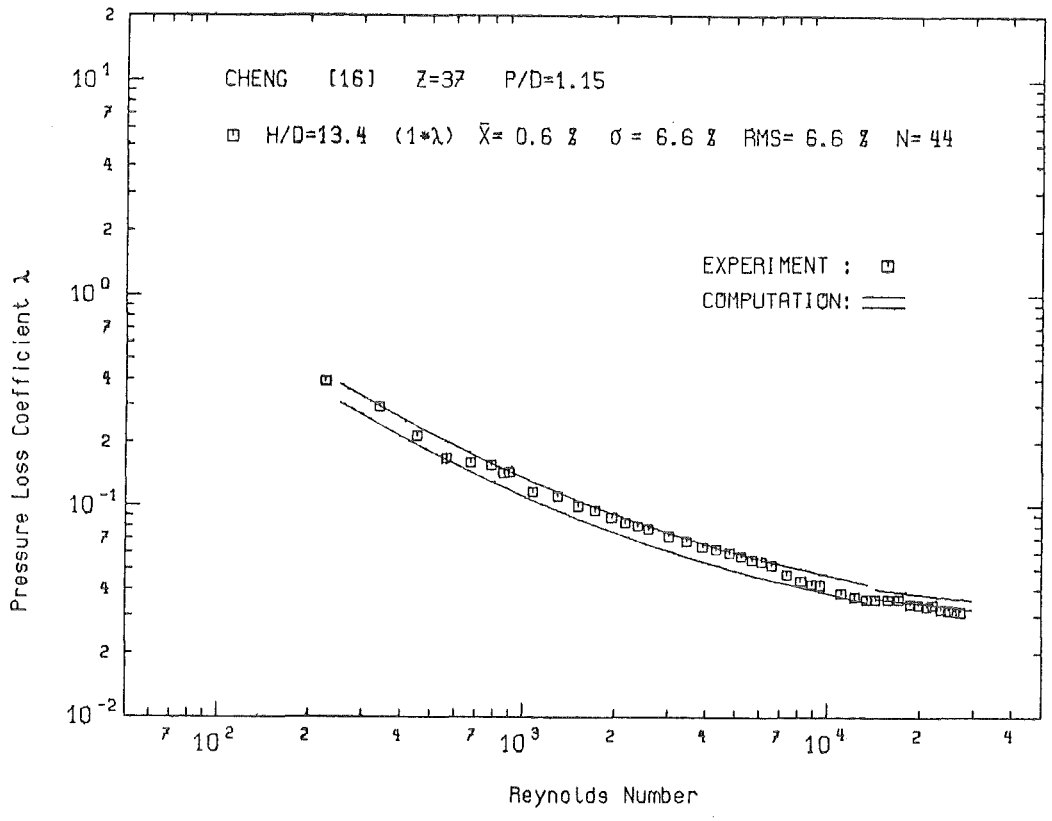

FIG.28 PRESSURE LOSS COEFFICIENT AS A FUNCTION OF THE REYNOLDS NUMBER EXPERIMENT AND COMPUTATION

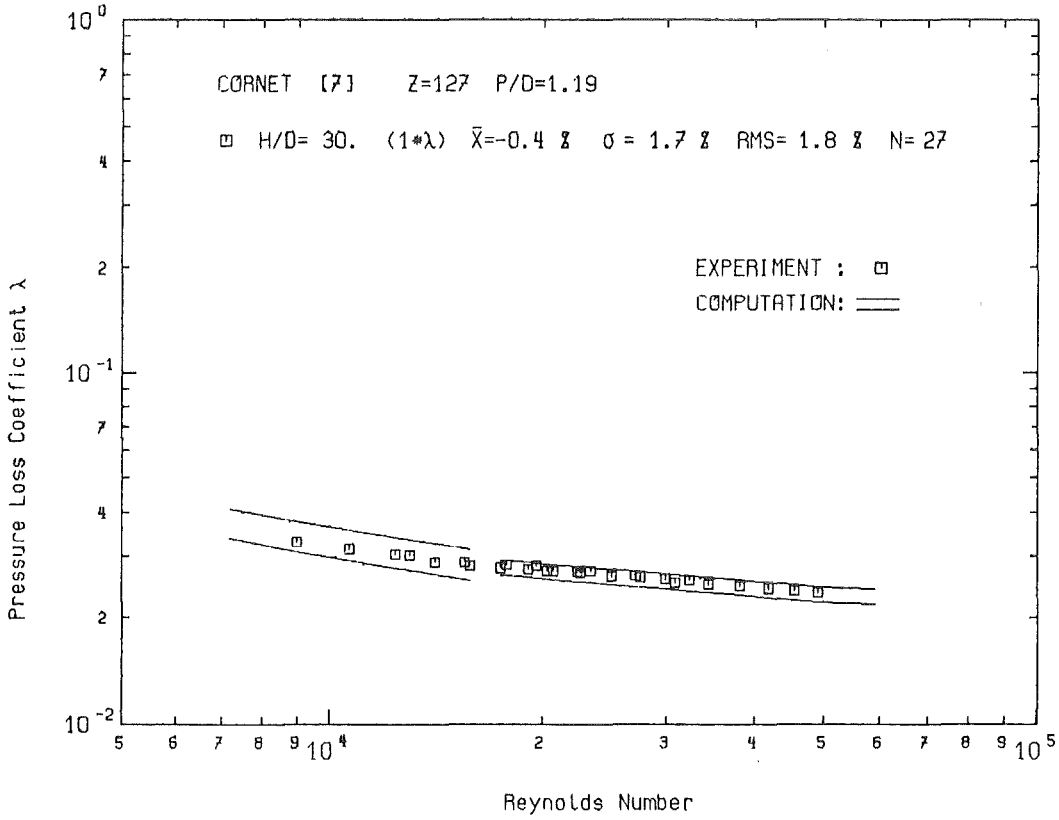

FIG.29 PRESSURE LOSS COEFFICIENT AS A FUNCTION OF THE REYNOLDS NUMBER EXPERIMENT AND COMPUTATION

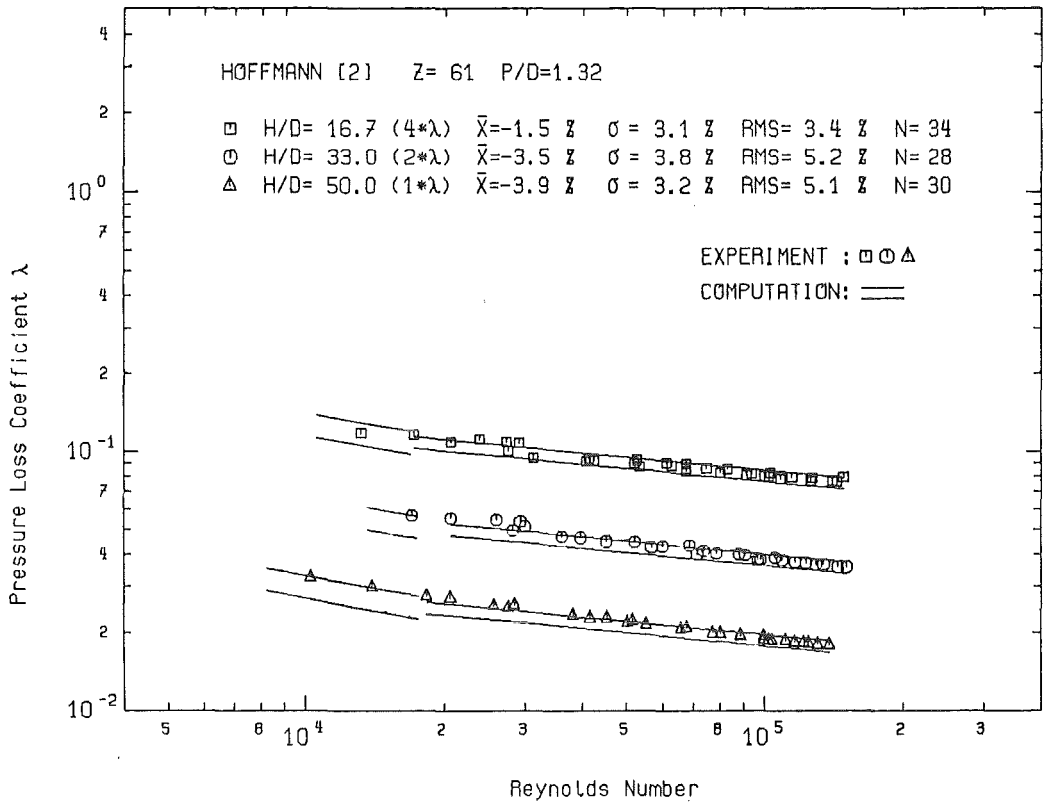

FIG.30 PRESSURE LOSS COEFFICIENT AS A FUNCTION OF THE REYNOLDS NUMBER EXPERIMENT AND COMPUTATION

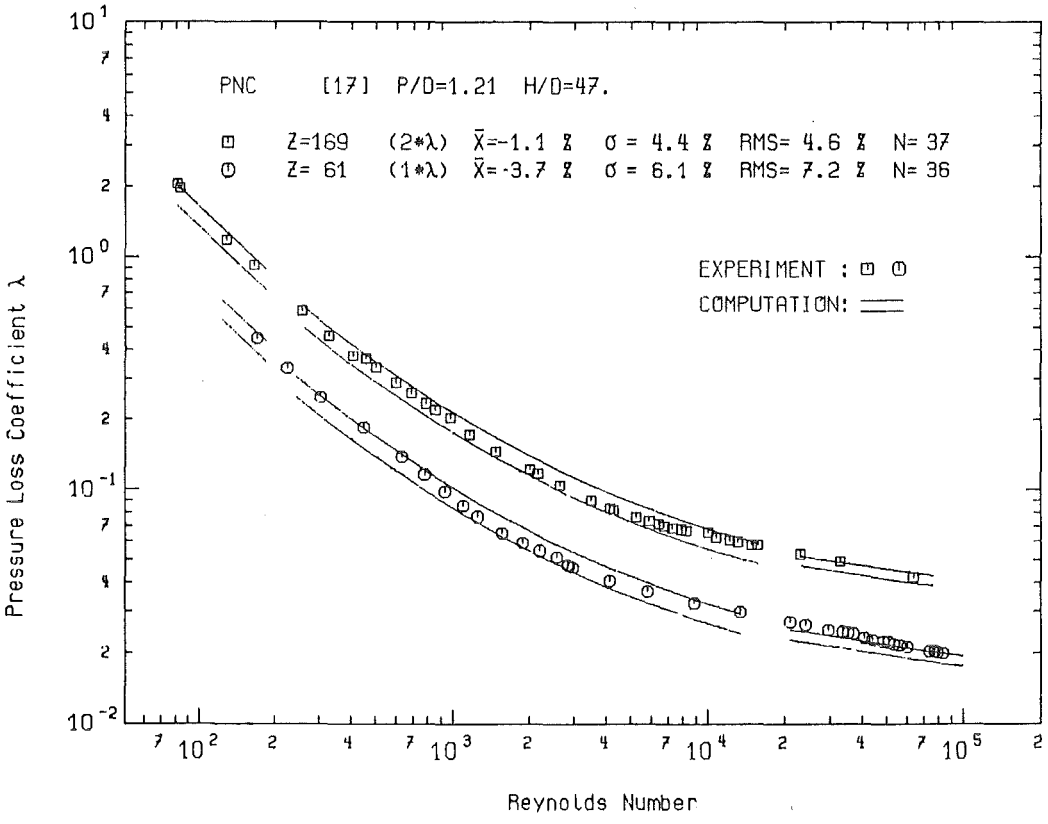

FIG.31 PRESSURE LOSS COEFFICIENT AS A FUNCTION OF THE REYNOLDS NUMBER EXPERIMENT AND COMPUTATION

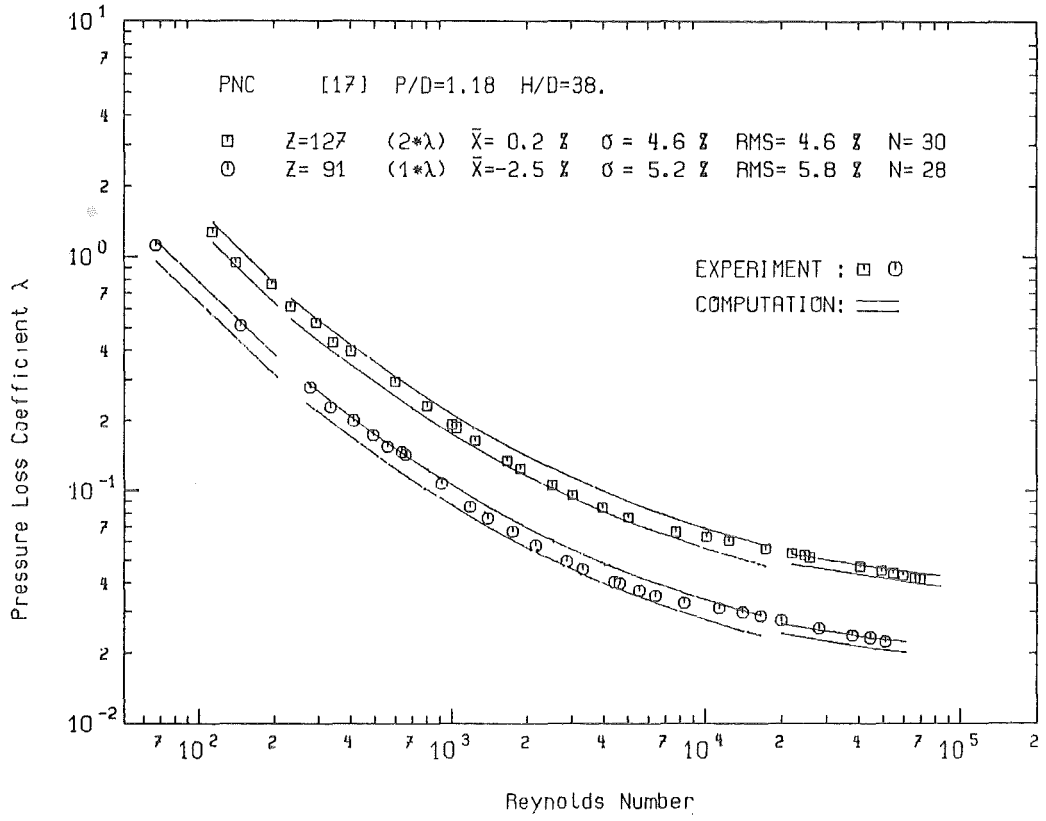

FIG.32 PRESSURE LOSS COEFFICIENT AS A FUNCTION OF THE REYNOLDS NUMBER EXPERIMENT AND COMPUTATION

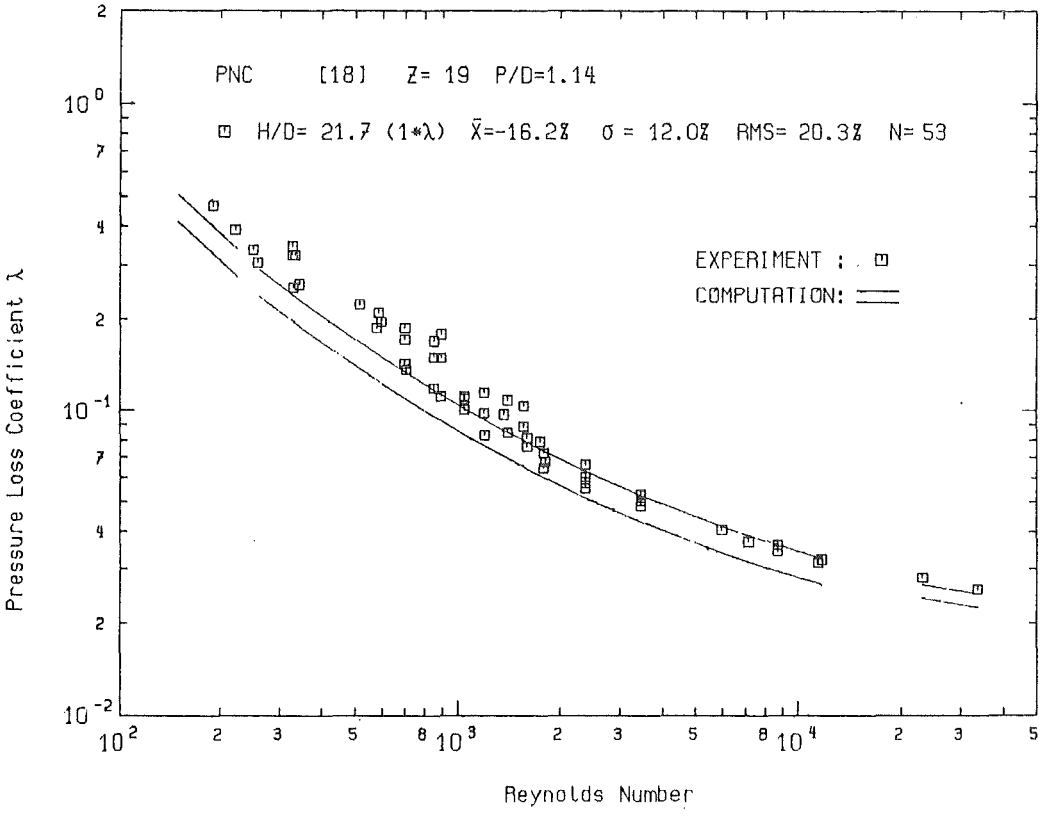

FIG.33 PRESSURE LOSS COEFFICIENT AS A FUNCTION OF THE REYNOLDS NUMBER EXPERIMENT AND COMPUTATION

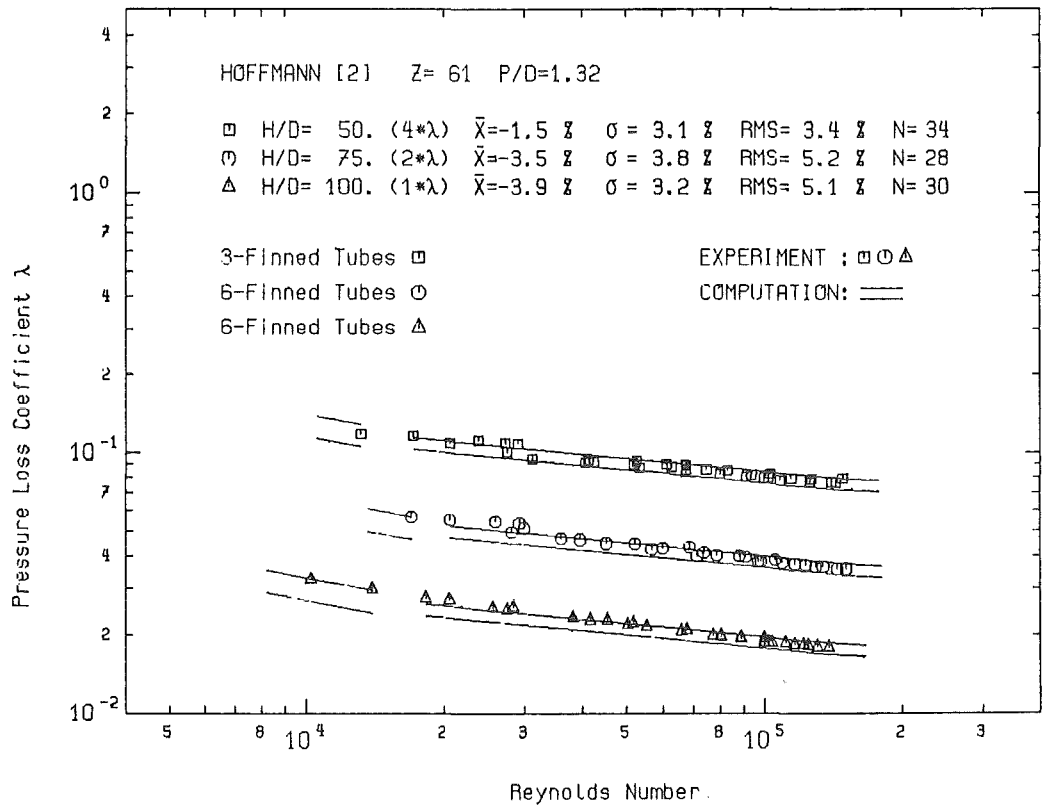

FIG.34 PRESSURE LOSS COEFFICIENT AS A FUNCTION OF THE REYNOLDS NUMBER EXPERIMENT AND COMPUTATION

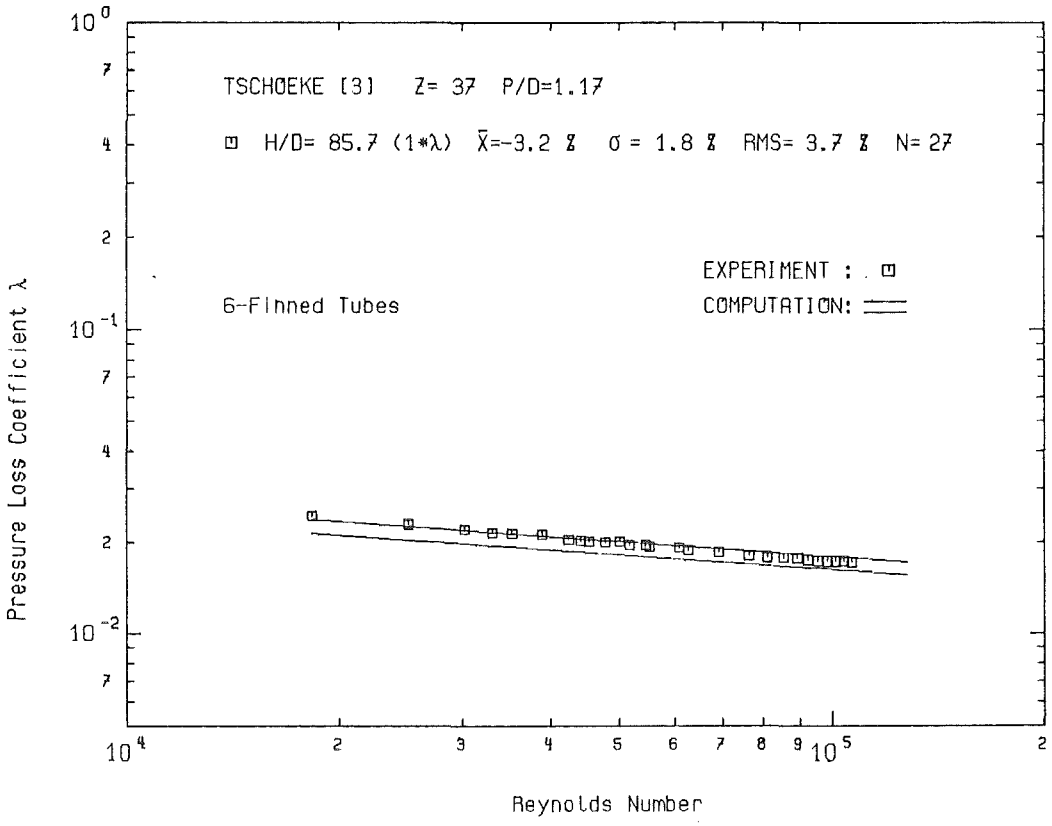

FIG.35 PRESSURE LOSS COEFFICIENT AS A FUNCTION OF THE REYNOLDS NUMBER EXPERIMENT AND COMPUTATION

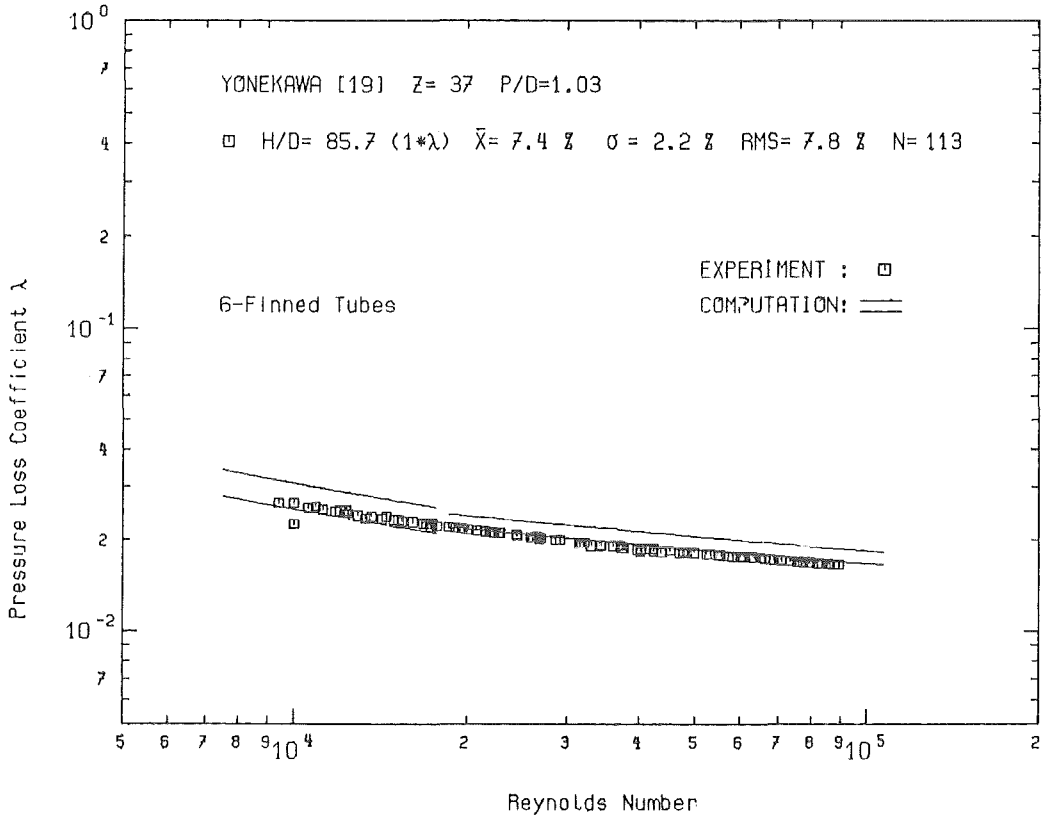

FIG.36 PRESSURE LOSS COEFFICIENT AS A FUNCTION OF THE REYNOLDS NUMBER EXPERIMENT AND COMPUTATION

ANNEX

MEASURED DATAS

TABLES A1-A12

	Re	λ		Re	λ		Re	λ
1	27.	1.22130	36	1106.	0.05544	71	5416.	0.03421
2	53.	0.62250	37	1118.	0.05580	72	5659.	0.03395
3	82.	0.40750	38	1133.	0.05790	73	6004.	0.03307
4	112.	0.29870	39	1158.	0.05836	74	6430.	0.03252
5	140.	0.24000	40	1186.	0.05901	75	6778.	0.03161
6	166.	0.20260	41	1223.	0.05884	76	7230.	0.03110
7	192.	0.17631	42	1246.	0.05867	77	7737.	0.03023
8	222.	0.15034	43	1270.	0.05857	78	8059.	0.02984
9	250.	0.13391	44	1295.	0.05806	79	8460.	0.02945
10	273.	0.12437	45	1350.	0.05749	80	8921.	0.02902
11	312.	0.10750	46	1376.	0.05697	81	9511.	0.02842
12	361.	0.09305	47	1428.	0.05676	82	9975.	0.02801
13	382.	0.08295	48	1481.	0.05600	83	10490.	0.02769
14	403.	0.07940	49	1529.	0.05567	84	10920.	0.02740
15	427.	0.07607	50	1658.	0.05591	85	11520.	0.02712
16	448.	0.07273	51	1754.	0.05470	86	12150.	0.02666
17	467.	0.07027	52	1860.	0.05377	87	12400.	0.02655
18	487.	0.06770	53	1974.	0.05245	88	12760.	0.02649
19	513.	0.06471	54	2184.	0.04992	89	13130.	0.02619
20	536.	0.06245	55	2307.	0.04862	90	13820.	0.02595
21	569.	0.05956	56	2472.	0.04733	91	14610.	0.02564
22	603.	0.05674	57	2598.	0.04619	92	15370.	0.02541
23	659.	0.05298	58	2776.	0.04508	93	16300.	0.02511
24	681.	0.05174	59	2954.	0.04355	94	17320.	0.02477
25	733.	0.04900	60	3029.	0.04315	95	18100.	0.02470
26	779.	0.04650	61	3104.	0.04283	96	19260.	0.02443
27	818.	0.04503	62	3315.	0.04194	97	20430.	0.02419
28	857.	0.04408	63	3474.	0.04098	98	21690.	0.02387
29	913.	0.04738	64	3650.	0.04006	99	22910.	0.02372
30	971.	0.04853	65	3888.	0.03926	100	23610.	0.02357
31	1008.	0.04978	66	4097.	0.03839	101	24820.	0.02352
32	1026.	0.05035	67	4366.	0.03753			
33	1051.	0.05194	68	4614.	0.03674			
34	1064.	0.05262	69	5070.	0.03541			
35	1096.	0.05482	70	5105.	0.03545			

TABLE A1: BUNDLE P/D = 1.02 H/D = 8.3

	Re	λ		Re	λ		Re	λ
1	8.	4.09240	36	997.	0.03948	71	3553.	0.04076
2	25.	1.27740	37	1003.	0.03833	72	3759.	0.03978
3	42.	0.77210	38	1021.	0.03838	73	4011.	0.03858
4	61.	0.54100	39	1046.	0.03758	74	4219.	0.03781
5	83.	0.39400	40	1060.	0.03684	75	4461.	0.03691
6	103.	0.31470	41	1075.	0.03938	76	4720.	0.03616
7	129.	0.25420	42	1104.	0.04499	77	5022.	0.03552
8	152.	0.21304	43	1133.	0.04785	78	5272.	0.03478
9	172.	0.19468	44	1166.	0.05001	79	5595.	0.03411
10	198.	0.16688	45	1195.	0.05222	80	6014.	0.03292
11	222.	0.14718	46	1220.	0.05381	81	6292.	0.03237
12	248.	0.13744	47	1240.	0.05523	82	6717.	0.03165
13	288.	0.11607	48	1265.	0.05686	83	7115.	0.03076
14	300.	0.11004	49	1290.	0.05865	84	7519.	0.03005
15	315.	0.10482	50	1318.	0.05894	85	7901.	0.02944
16	336.	0.09908	51	1343.	0.05860	86	8422.	0.02869
17	355.	0.09352	52	1360.	0.05896	87	8872.	0.02800
18	379.	0.08847	53	1413.	0.05786	88	9350.	0.02756
19	405.	0.08325	54	1466.	0.05700	89	9956.	0.02684
20	420.	0.08052	55	1512.	0.05698	90	10610.	0.02651
21	446.	0.07633	56	1558.	0.05641	91	11280.	0.02595
22	473.	0.07205	57	1586.	0.05626	92	11880.	0.02562
23	497.	0.06939	58	1684.	0.05478	93	12570.	0.02524
24	527.	0.06582	59	1780.	0.05414	94	13270.	0.02481
25	557.	0.06312	60	1897.	0.05232	95	14150.	0.02442
26	614.	0.05779	61	1997.	0.05137	96	15010.	0.02417
27	628.	0.05688	62	2116.	0.05014	97	15900.	0.02393
28	672.	0.05378	63	2250.	0.04879	98	16780.	0.02353
29	710.	0.05104	64	2385.	0.04934	99	17820.	0.02319
30	751.	0.04889	65	2536.	0.04755	100	18680.	0.02297
31	791.	0.04672	66	2679.	0.04633	101	19890.	0.02269
32	838.	0.04490	67	2833.	0.04510	102	21080.	0.02245
33	890.	0.04230	68	3031.	0.04386	103	22390.	0.02215
34	945.	0.04092	69	3185.	0.04270	104	23570.	0.02195
35	947.	0.04036	70	3350.	0.04158	105	24940.	0.02182
						106	25490.	0.02168

TABLE A2: BUNDLE P/D = 1.02 H/D = 12.5

	Re	λ		Re	λ		Re	λ
1	19.	1.88190	36	1040.	0.04474	71	5297.	0.03423
2	44.	0.74950	37	1058.	0.04567	72	5644.	0.03311
3	71.	0.47110	38	1082.	0.04729	73	5995.	0.03270
4	102.	0.32420	39	1109.	0.05053	74	6291.	0.03219
5	128.	0.26100	40	1122.	0.05306	75	6692.	0.03119
6	155.	0.21570	41	1139.	0.05406	76	7095.	0.03051
7	180.	0.18785	42	1153.	0.05686	77	7499.	0.02999
8	207.	0.16307	43	1174.	0.05678	78	7901.	0.02963
9	231.	0.14746	44	1203.	0.05908	79	8413.	0.02875
10	259.	0.13099	45	1217.	0.05788	80	8902.	0.02822
11	291.	0.11540	46	1250.	0.05908	81	9481.	0.02787
12	317.	0.10648	47	1305.	0.05857	82	9988.	0.02728
13	340.	0.10074	48	1334.	0.05865	83	10570.	0.02679
14	364.	0.09446	49	1376.	0.05796	84	11220.	0.02625
15	375.	0.08797	50	1421.	0.05790	85	11970.	0.02593
16	401.	0.08147	51	1584.	0.05596	86	12600.	0.02546
17	421.	0.08223	52	1687.	0.05484	87	13320.	0.02510
18	447.	0.07659	53	1781.	0.05365	88	13970.	0.02477
19	471.	0.07198	54	1807.	0.05309	89	14970.	0.02417
20	499.	0.06966	55	2018.	0.05105	90	15840.	0.02378
21	505.	0.07172	56	2171.	0.04949	91	16730.	0.02350
22	526.	0.06757	57	2362.	0.04746	92	17700.	0.02313
23	560.	0.06342	58	2569.	0.04570	93	18720.	0.02296
24	605.	0.05894	59	2673.	0.04544	94	19990.	0.02259
25	643.	0.05402	60	2807.	0.04433	95	20970.	0.02239
26	707.	0.04982	61	2969.	0.04374	96	22300.	0.02204
27	759.	0.04611	62	3155.	0.04288	97	23620.	0.02179
28	807.	0.04484	63	3342.	0.04142	98	25070.	0.02150
29	861.	0.04330	64	3556.	0.04062	99	26570.	0.02121
30	879.	0.04206	65	3771.	0.03960	100	28030.	0.02088
31	920.	0.04144	66	4012.	0.03863	101	29900.	0.02060
32	933.	0.04109	67	4225.	0.03714	102	31110.	0.02061
33	955.	0.04076	68	4466.	0.03694	103	32780.	0.02030
34	997.	0.04201	69	4734.	0.03592			
35	1011.	0.04289	70	5001.	0.03505			

TABLE A3: BUNDLE P/D = 1.02 H/D = 16.7

	Re	λ		Re	λ		Re	λ
1	39.	1.18280	51	3571.	0.05046	101	17247.	0.03335
2	60.	0.75240	52	3578.	0.05100	102	17482.	0.03340
3	83.	0.54450	53	3741.	0.04783	103	17592.	0.03319
4	96.	0.46840	54	3867.	0.04819	104	17942.	0.03325
5	116.	0.39050	55	3914.	0.04924	105	19403.	0.03277
6	132.	0.34300	56	4207.	0.04808	106	19791.	0.03267
7	146.	0.31310	57	4254.	0.04771	107	19907.	0.03257
8	154.	0.30260	58	4355.	0.04645	108	20281.	0.03263
9	162.	0.27990	59	5005.	0.04444	109	20689.	0.03196
10	175.	0.21080	60	5188.	0.04488	110	21035.	0.03211
11	181.	0.25180	61	5282.	0.04406	111	21666.	0.03221
12	195.	0.21626	62	5345.	0.04402	112	22207.	0.03202
13	197.	0.21077	63	6047.	0.04262	113	22250.	0.03196
14	207.	0.21710	64	6110.	0.04225	114	22646.	0.03196
15	224.	0.19890	65	6372.	0.04253	115	22646.	0.03183
16	256.	0.17710	66	6674.	0.04074	116	23350.	0.03167
17	271.	0.16420	67	6839.	0.04155	117	23953.	0.03174
18	286.	0.16250	68	6998.	0.04054	118	24550.	0.03126
19	298.	0.16006	69	7269.	0.04048	119	24827.	0.03115
20	315.	0.15000	70	7418.	0.04060	120	25151.	0.03118
21	354.	0.12990	71	7797.	0.03969	121	25151.	0.03135
22	361.	0.13370	72	7890.	0.03915	122	25242.	0.03118
23	364.	0.13017	73	8249.	0.03662	123	25599.	0.03112
24	415.	0.12030	74	8250.	0.03952	124	26389.	0.03116
25	426.	0.11171	75	8414.	0.03980	125	26446.	0.03099
26	454.	0.11047	76	8623.	0.03854	126	26912.	0.03089
27	467.	0.10920	77	8839.	0.03830	127	28870.	0.03068
28	509.	0.10050	78	8950.	0.03871	128	28965.	0.03044
29	516.	0.10190	79	9014.	0.03843	129	29440.	0.03049
30	550.	0.10031	80	9451.	0.03812	130	29659.	0.03029
31	601.	0.10920	81	9637.	0.03792	131	30560.	0.03056
32	616.	0.11194	82	10082.	0.03749	132	30560.	0.03071
33	661.	0.10740	83	10240.	0.03737	133	31549.	0.03023
34	687.	0.11061	84	10508.	0.03718	134	32011.	0.02996
35	705.	0.11022	85	10725.	0.03697	135	33210.	0.02944
36	718.	0.10764	86	10726.	0.03663	136	33656.	0.02961
37	765.	0.10624	87	10995.	0.03674	137	34316.	0.02973
38	782.	0.10684	88	11267.	0.03651	138	34629.	0.02950
39	857.	0.10099	89	12370.	0.03565	139	37362.	0.02888
40	865.	0.10116	90	12621.	0.03619	140	37862.	0.02903
41	897.	0.10146	91	12759.	0.03563	141	41657.	0.02857
42	1002.	0.09576	92	12871.	0.03539	142	42209.	0.02835
43	1024.	0.09368	93	13194.	0.03506	143	45973.	0.02796
44	1419.	0.07904	94	13456.	0.03496	144	46575.	0.02786
45	1814.	0.07019	95	15016.	0.03423	145	47689.	0.02791
46	2134.	0.06445	96	15079.	0.03432	146	50483.	0.02771
47	2482.	0.05988	97	15393.	0.03431	147	53671.	0.02735
48	2849.	0.05611	98	15930.	0.03400	148	55043.	0.02720
49	3212.	0.05298	99	16498.	0.03254	149	59636.	0.02677
50	3476.	0.05135	100	16828.	0.03385	150	61166.	0.02679
						151	67101.	0.02627

TABLE A4: BUNDLE P/D = 1.04 H/D = 8.3

	Re	λ		Re	λ		Re	λ
1	33.	1.01780	51	2320.	0.05692	101	14500.	0.03073
2	52.	0.74430	52	2420.	0.05566	102	15400.	0.03073
3	76.	0.52070	53	2520.	0.05530	103	16170.	0.02992
4	101.	0.38920	54	2530.	0.05407	104	16500.	0.03020
5	119.	0.34330	55	2690.	0.05243	105	16600.	0.02985
6	129.	0.31910	56	2700.	0.05144	106	17900.	0.02945
7	142.	0.30130	57	2720.	0.05241	107	17900.	0.02915
8	149.	0.28490	58	2930.	0.05020	108	18300.	0.02963
9	153.	0.26700	59	3010.	0.04934	109	18500.	0.02948
10	160.	0.26010	60	3080.	0.04880	110	18700.	0.02939
11	168.	0.24650	61	3260.	0.05615	111	20200.	0.02888
12	176.	0.23320	62	3380.	0.04671	112	20400.	0.02887
13	197.	0.21200	63	3460.	0.04630	113	20750.	0.02889
14	219.	0.19160	64	3700.	0.04482	114	20900.	0.02882
15	238.	0.17950	65	3700.	0.04399	115	21300.	0.02847
16	272.	0.15900	66	3750.	0.04468	116	22400.	0.02853
17	318.	0.14090	67	4000.	0.04410	117	22500.	0.02844
18	359.	0.12680	68	4140.	0.04280	118	23100.	0.02825
19	419.	0.11120	69	4220.	0.04114	119	23100.	0.02830
20	455.	0.10440	70	4391.	0.04172	120	25000.	0.02765
21	493.	0.09860	71	4680.	0.04154	121	25360.	0.02779
22	526.	0.09371	72	4700.	0.04054	122	25500.	0.02781
23	567.	0.08913	73	5500.	0.03845	123	26900.	0.02746
24	624.	0.09316	74	5560.	0.03912	124	27700.	0.02736
25	682.	0.09900	75	6120.	0.03785	125	28100.	0.02731
26	737.	0.10190	76	6300.	0.03677	126	29000.	0.02706
27	763.	0.09957	77	6650.	0.03693	127	29700.	0.02696
28	786.	0.10250	78	6800.	0.03612	128	30200.	0.02692
29	796.	0.09945	79	7030.	0.03638	129	31100.	0.02679
30	814.	0.10130	80	7500.	0.03498	130	33200.	0.02649
31	850.	0.09754	81	7800.	0.03429	131	34200.	0.02605
32	863.	0.09639	82	7810.	0.03298	132	35400.	0.02610
33	898.	0.09697	83	8200.	0.03427	133	38200.	0.02561
34	916.	0.09454	84	8360.	0.03473	134	42700.	0.02495
35	1010.	0.09036	85	8550.	0.03405	135	47600.	0.02463
36	1010.	0.09170	86	8960.	0.03414	136	52300.	0.02405
37	1070.	0.08731	87	9000.	0.03355	137	52500.	0.02412
38	1110.	0.08744	88	9400.	0.03338	138	56500.	0.02382
39	1140.	0.08445	89	9780.	0.03340	139	57700.	0.02364
40	1170.	0.08492	90	9800.	0.03304	140	61900.	0.02337
41	1250.	0.08168	91	10300.	0.03277	141	62100.	0.02338
42	1310.	0.07759	92	10600.	0.03290	142	65800.	0.02312
43	1350.	0.07808	93	10950.	0.03268	143	66600.	0.02305
44	1400.	0.07594	94	11800.	0.03217	144	71100.	0.02276
45	1550.	0.07113	95	12300.	0.03201	145	71200.	0.02280
46	1690.	0.06839	96	12400.	0.03165	146	75500.	0.02248
47	1730.	0.06740	97	13400.	0.03130	147	76300.	0.02245
48	1930.	0.06330	98	13900.	0.03118	148	79600.	0.02226
49	2060.	0.06092	99	14100.	0.03050			
50	2110.	0.06022	100	14400.	0.03078			

TABLE A5: BUNDLE P/D = 1.04 H/D = 12.6

	Re	λ		Re	λ		Re	λ
1	29.	1.38200	41	4076.	0.04107	81	25900.	0.02571
2	50.	0.84310	42	5390.	0.03703	82	26900.	0.02578
3	70.	0.61500	43	6040.	0.03532	83	27000.	0.02565
4	85.	0.53070	44	6360.	0.03506	84	27500.	0.02546
5	100.	0.44830	45	7080.	0.03401	85	29000.	0.02526
6	111.	0.40810	46	7820.	0.03370	86	29100.	0.02529
7	132.	0.34070	47	7990.	0.03266	87	30000.	0.02507
8	141.	0.32540	48	8350.	0.03229	88	30700.	0.02521
9	161.	0.28470	49	8810.	0.03211	89	32450.	0.02477
10	184.	0.25300	50	9040.	0.03165	90	32570.	0.02481
11	201.	0.23820	51	10200.	0.03079	91	33400.	0.02459
12	262.	0.17840	52	10300.	0.03099	92	34500.	0.02461
13	323.	0.15000	53	10800.	0.03100	93	34700.	0.02439
14	388.	0.12630	54	10840.	0.03034	94	35050.	0.02443
15	431.	0.11710	55	11240.	0.03007	95	36300.	0.02423
16	478.	0.10300	56	11500.	0.03008	96	37750.	0.02413
17	521.	0.09573	57	12500.	0.02948	97	38350.	0.02418
18	589.	0.08515	58	12900.	0.02942	98	38400.	0.02395
19	650.	0.08668	59	13000.	0.02930	99	40800.	0.02381
20	701.	0.09947	60	13580.	0.02912	100	41500.	0.02380
21	774.	0.10120	61	13800.	0.02878	101	43000.	0.02365
22	854.	0.09854	62	14200.	0.02892	102	44100.	0.02362
23	916.	0.09505	63	14700.	0.02856	103	45500.	0.02341
24	976.	0.09288	64	15060.	0.02874	104	46900.	0.02338
25	1050.	0.08921	65	15460.	0.02844	105	48300.	0.02319
26	1110.	0.08418	66	15500.	0.02817	106	50450.	0.02305
27	1130.	0.08581	67	16180.	0.02792	107	51300.	0.02285
28	1200.	0.08359	68	16500.	0.02817	108	53400.	0.02283
29	1250.	0.07908	69	16700.	0.02779	109	54300.	0.02261
30	1460.	0.07219	70	17590.	0.02783	110	57400.	0.02248
31	1670.	0.06691	71	18100.	0.02741	111	57400.	0.02246
32	1950.	0.06191	72	18100.	0.02758	112	60800.	0.02222
33	2130.	0.05839	73	20450.	0.02707	113	61000.	0.02224
34	2370.	0.05503	74	20770.	0.02680	114	63400.	0.02205
35	2520.	0.05306	75	20900.	0.02667	115	65100.	0.02197
36	2760.	0.05030	76	21100.	0.02661	116	67300.	0.02179
37	3050.	0.04790	77	23100.	0.02628	117	69500.	0.02168
38	3330.	0.04563	78	23800.	0.02632	118	72000.	0.02144
39	3650.	0.04369	79	24400.	0.02606	119	75660.	0.02132
40	4020.	0.04173	80	24500.	0.02601			

TABLE A6: BUNDLE P/D = 1.04 H/D = 17.0

	Re	λ		Re	λ		Re	λ
1	49.	1.49910	51	1660.	0.09426	101	23100.	0.03920
2	65.	1.04950	52	1953.	0.08681	102	23210.	0.03900
3	67.	1.05290	53	2258.	0.08042	103	23210.	0.03880
4	89.	0.78886	54	2552.	0.07568	104	24180.	0.03868
5	97.	0.73209	55	2845.	0.07187	105	25440.	0.03843
6	105.	0.63534	56	3116.	0.06678	106	25790.	0.03834
7	123.	0.54825	57	3555.	0.06516	107	25790.	0.03805
8	133.	0.50684	58	3575.	0.06629	108	26000.	0.03813
9	143.	0.47577	59	3986.	0.06182	109	26850.	0.03818
10	152.	0.45741	60	4262.	0.06023	110	27400.	0.03787
11	160.	0.42702	61	4568.	0.05749	111	28620.	0.03771
12	174.	0.31980	62	4767.	0.05814	112	28620.	0.03743
13	176.	0.36432	63	4990.	0.05691	113	28880.	0.03778
14	177.	0.38732	64	5111.	0.05692	114	29560.	0.03763
15	195.	0.35591	65	5710.	0.05337	115	30950.	0.03734
16	199.	0.29291	66	5750.	0.05701	116	31360.	0.03725
17	204.	0.32594	67	5958.	0.05380	117	31360.	0.03708
18	217.	0.31939	68	6852.	0.05026	118	32140.	0.03707
19	221.	0.26700	69	7150.	0.05056	119	32320.	0.03714
20	239.	0.27932	70	7743.	0.04868	120	34280.	0.03664
21	246.	0.24994	71	7994.	0.04848	121	34280.	0.03654
22	277.	0.23029	72	8342.	0.04829	122	34660.	0.03681
23	281.	0.25412	73	8499.	0.04726	123	34900.	0.03679
24	307.	0.21625	74	9091.	0.04643	124	35130.	0.03658
25	309.	0.22738	75	9581.	0.04661	125	36730.	0.03635
26	338.	0.22449	76	9990.	0.04553	126	37250.	0.03624
27	360.	0.20720	77	10220.	0.04533	127	37250.	0.03603
28	376.	0.21296	78	10220.	0.04475	128	38160.	0.03615
29	418.	0.19940	79	11360.	0.04397	129	40100.	0.03597
30	423.	0.19930	80	11550.	0.04513	130	40260.	0.03581
31	474.	0.19294	81	11980.	0.04389	131	40260.	0.03561
32	487.	0.18629	82	12780.	0.04338	132	41070.	0.03587
33	525.	0.18627	83	12780.	0.04280	133	43130.	0.03543
34	548.	0.17587	84	13640.	0.04240	134	43520.	0.03534
35	584.	0.17378	85	14370.	0.04214	135	43520.	0.03516
36	619.	0.16545	86	14990.	0.04205	136	43890.	0.03524
37	661.	0.15607	87	15330.	0.04170	137	45050.	0.03529
38	697.	0.15539	88	15330.	0.04132	138	49600.	0.03462
39	752.	0.14758	89	16770.	0.04097	139	49600.	0.03439
40	761.	0.14452	90	17278.	0.04089	140	49820.	0.03473
41	767.	0.14655	91	17330.	0.04110	141	53180.	0.03430
42	787.	0.14578	92	17970.	0.04055	142	62830.	0.03361
43	872.	0.13688	93	17970.	0.04027	143	73160.	0.03276
44	955.	0.12855	94	18180.	0.04027	144	83590.	0.03205
45	995.	0.12722	95	19250.	0.04014	145	93740.	0.03160
46	1114.	0.11945	96	20080.	0.03960			
47	1168.	0.11449	97	20540.	0.03966			
48	1256.	0.11158	98	20540.	0.03953			
49	1360.	0.10664	99	21660.	0.03923			
50	1427.	0.10244	100	22730.	0.03891			

TABLE A7: BUNDLE P/D = 1.07 H/D = 8.3

	Re	λ		Re	λ		Re	λ
1	31.	1.78700	61	11864.	0.03560	121	32172.	0.02982
2	73.	0.73030	62	12147.	0.03627	122	32185.	0.02973
3	119.	0.45800	63	12147.	0.03540	123	32322.	0.02974
4	146.	0.38190	64	12374.	0.03562	124	32594.	0.02950
5	168.	0.33210	65	12547.	0.03511	125	32621.	0.02963
6	185.	0.30320	66	12917.	0.03508	126	32750.	0.02956
7	206.	0.27220	67	13505.	0.03509	127	32750.	0.02962
8	238.	0.24430	68	13570.	0.03474	128	32907.	0.02960
9	259.	0.23240	69	13768.	0.03469	129	33219.	0.02934
10	267.	0.22350	70	13768.	0.03419	130	33219.	0.02957
11	303.	0.20530	71	13969.	0.03468	131	33850.	0.02948
12	379.	0.19070	72	14439.	0.03424	132	35592.	0.02921
13	438.	0.17700	73	15734.	0.03389	133	36017.	0.02916
14	513.	0.16780	74	15831.	0.03393	134	36098.	0.02931
15	601.	0.15300	75	16767.	0.03350	135	36364.	0.02933
16	685.	0.13990	76	17085.	0.03344	136	36599.	0.02922
17	759.	0.13150	77	17165.	0.03377	137	37122.	0.02898
18	839.	0.12440	78	17223.	0.03316	138	37640.	0.02891
19	924.	0.11620	79	17324.	0.03334	139	37964.	0.02885
20	1010.	0.11600	80	17726.	0.03304	140	38145.	0.02899
21	1069.	0.10623	81	18006.	0.03297	141	38324.	0.02887
22	1092.	0.10540	82	18006.	0.03289	142	38329.	0.02878
23	1211.	0.09829	83	18358.	0.03282	143	38870.	0.02889
24	1264.	0.09576	84	18358.	0.03277	144	38870.	0.02884
25	1294.	0.09411	85	18535.	0.03270	145	39415.	0.02882
26	1372.	0.09107	86	19162.	0.03259	146	40292.	0.02870
27	1457.	0.08704	87	19735.	0.03217	147	40337.	0.02885
28	1746.	0.07754	88	20257.	0.03219	148	41035.	0.02854
29	2038.	0.07149	89	21636.	0.03187	149	41878.	0.02852
30	2324.	0.06605	90	21659.	0.03187	150	41907.	0.02849
31	2652.	0.06119	91	22069.	0.03169	151	42267.	0.02829
32	2973.	0.05771	92	22273.	0.03175	152	42855.	0.02836
33	3255.	0.05520	93	22273.	0.03177	153	43728.	0.02824
34	3606.	0.05263	94	22616.	0.03166	154	43932.	0.02822
35	3864.	0.05091	95	22616.	0.03145	155	44038.	0.02837
36	4235.	0.04906	96	22893.	0.03142	156	44138.	0.02833
37	4284.	0.04959	97	22947.	0.03156	157	44469.	0.02829
38	4523.	0.04754	98	22947.	0.03136	158	44546.	0.02810
39	4550.	0.04769	99	23281.	0.03144	159	44753.	0.02822
40	4590.	0.04713	100	23764.	0.03120	160	45500.	0.02822
41	4590.	0.04612	101	23952.	0.03122	161	48674.	0.02781
42	4679.	0.04802	102	25000.	0.03103	162	49833.	0.02770
43	4679.	0.04613	103	26225.	0.03088	163	53266.	0.02738
44	4836.	0.04677	104	26472.	0.03090	164	53345.	0.02738
45	4940.	0.04608	105	27097.	0.03062	165	54341.	0.02725
46	5820.	0.04489	106	27349.	0.03057	166	57753.	0.02706
47	6951.	0.04156	107	27349.	0.03053	167	58688.	0.02699
48	7493.	0.04075	108	27406.	0.03040	168	62495.	0.02674
49	7840.	0.03879	109	27537.	0.03054	169	63035.	0.02666
50	8070.	0.03982	110	27669.	0.03044	170	67110.	0.02628
51	8568.	0.03864	111	27669.	0.03033	171	67382.	0.02632
52	9046.	0.03824	112	27820.	0.03041	172	67529.	0.02628
53	9179.	0.03793	113	27894.	0.03040	173	71500.	0.02593
54	9179.	0.03807	114	28071.	0.03037	174	72013.	0.02597
55	9179.	0.03759	115	28108.	0.03086	175	72485.	0.02595
56	9313.	0.03791	116	28743.	0.03024	176	75590.	0.02581
57	9626.	0.03753	117	30266.	0.02991	177	77000.	0.02568
58	10277.	0.03694	118	30897.	0.03003	178	77258.	0.02571
59	11364.	0.03639	119	31285.	0.03006	179	82307.	0.02545
60	11800.	0.03485	120	31904.	0.02968	180	88568.	0.02503

TABLE A8: BUNDLE P/D = 1.07 H/D = 12.5

	Re	λ		Re	λ		Re	λ
1	61.	0.81550	46	908.	0.10835	91	22649.	0.02871
2	87.	0.59750	47	972.	0.10409	92	22812.	0.02880
3	102.	0.52560	48	1002.	0.10184	93	22947.	0.02910
4	119.	0.46250	49	1072.	0.09704	94	25033.	0.02849
5	142.	0.39465	50	1079.	0.09670	95	25242.	0.02838
6	154.	0.36447	51	1422.	0.08154	96	25775.	0.02815
7	162.	0.32706	52	1547.	0.08130	97	26423.	0.02813
8	172.	0.33168	53	1750.	0.07300	98	27669.	0.02786
9	176.	0.30917	54	1895.	0.06795	99	28761.	0.02762
10	180.	0.26025	55	2142.	0.06424	100	29975.	0.02748
11	181.	0.30936	56	2367.	0.05968	101	30727.	0.02740
12	192.	0.26626	57	2502.	0.05858	102	31637.	0.02717
13	195.	0.29601	58	2628.	0.05633	103	32594.	0.02705
14	198.	0.29571	59	2904.	0.05373	104	34513.	0.02674
15	211.	0.29653	60	2985.	0.05230	105	35089.	0.02654
16	220.	0.25078	61	3260.	0.05061	106	35120.	0.02665
17	223.	0.25722	62	3434.	0.04891	107	37389.	0.02639
18	232.	0.27507	63	3587.	0.04804	108	37608.	0.02639
19	236.	0.23656	64	3785.	0.04682	109	39506.	0.02609
20	248.	0.27136	65	3956.	0.04562	110	40265.	0.02605
21	259.	0.22983	66	4178.	0.04468	111	40337.	0.02602
22	266.	0.25964	67	4311.	0.04417	112	43114.	0.02571
23	267.	0.20141	68	4634.	0.04265	113	43141.	0.02573
24	278.	0.21270	69	5703.	0.03990	114	43895.	0.02557
25	289.	0.21953	70	6984.	0.03791	115	46017.	0.02536
26	289.	0.22468	71	8555.	0.03519	116	48285.	0.02514
27	303.	0.20491	72	8808.	0.03453	117	49096.	0.02505
28	331.	0.19251	73	9268.	0.03475	118	52206.	0.02471
29	343.	0.18678	74	10527.	0.03432	119	52845.	0.02486
30	368.	0.18191	75	11406.	0.03325	120	57340.	0.02445
31	370.	0.16909	76	11584.	0.03311	121	57425.	0.02435
32	435.	0.15264	77	12928.	0.03229	122	61927.	0.02392
33	455.	0.14659	78	13210.	0.03197	123	62045.	0.02401
34	506.	0.14832	79	13835.	0.03205	124	66514.	0.02372
35	550.	0.13897	80	14257.	0.03141	125	66682.	0.02362
36	575.	0.13707	81	15350.	0.03141	126	71101.	0.02332
37	624.	0.13124	82	16140.	0.03095	127	71583.	0.02334
38	642.	0.13336	83	17109.	0.03033	128	75688.	0.02304
39	708.	0.12947	84	17620.	0.03029	129	76533.	0.02300
40	737.	0.12276	85	17712.	0.03056	130	80020.	0.02282
41	792.	0.11777	86	18358.	0.03017	131	81545.	0.02273
42	809.	0.11738	87	19960.	0.02955	132	88883.	0.02235
43	815.	0.11607	88	20169.	0.02974			
44	887.	0.11155	89	20653.	0.02948			
45	889.	0.11032	90	22020.	0.02900			

TABLE A9: BUNDLE P/D = 1.07 H/D = 16.7

	Re	λ		Re	λ		Re	λ
1	42.	2.06090	41	4452.	0.06778	81	29935.	0.04474
2	55.	1.59770	42	4838.	0.06578	82	31533.	0.04447
3	77.	1.06440	43	5995.	0.06543	83	31913.	0.04420
4	98.	0.80484	44	6440.	0.06285	84	31960.	0.04403
5	110.	0.73247	45	7781.	0.05780	85	32992.	0.04412
6	134.	0.61239	46	8311.	0.05749	86	34275.	0.04358
7	147.	0.53993	47	9376.	0.05523	87	34659.	0.04387
8	158.	0.52074	48	9810.	0.05484	88	35040.	0.04352
9	184.	0.43844	49	10365.	0.05199	89	36222.	0.04357
10	204.	0.40591	50	10726.	0.05321	90	36815.	0.04319
11	206.	0.35482	51	11468.	0.05285	91	37227.	0.04337
12	247.	0.35771	52	12037.	0.05209	92	37525.	0.04332
13	281.	0.30306	53	12746.	0.05161	93	39354.	0.04279
14	295.	0.31303	54	12937.	0.05144	94	39670.	0.04301
15	352.	0.26562	55	14085.	0.05045	95	39682.	0.04284
16	404.	0.25419	56	14374.	0.05030	96	41927.	0.04263
17	466.	0.24349	57	14826.	0.04930	97	42274.	0.04251
18	543.	0.21927	58	15506.	0.04941	98	45256.	0.04215
19	632.	0.18954	59	16103.	0.04922	99	47837.	0.04190
20	706.	0.17538	60	16442.	0.04924	100	50907.	0.04154
21	770.	0.16691	61	17509.	0.04842	101	53653.	0.04133
22	847.	0.15572	62	17520.	0.04842	102	57088.	0.04090
23	919.	0.14612	63	18791.	0.04757	103	59792.	0.04072
24	992.	0.14030	64	19122.	0.04787	104	63584.	0.04036
25	1006.	0.14053	65	19341.	0.04768	105	66811.	0.04017
26	1078.	0.13532	66	20635.	0.04715	106	70467.	0.03979
27	1158.	0.12831	67	21204.	0.04652	107	73285.	0.03957
28	1266.	0.12338	68	21282.	0.04694	108	75791.	0.03939
29	1289.	0.12208	69	22194.	0.04677	109	80973.	0.03898
30	1375.	0.11729	70	23140.	0.04634	110	87084.	0.03855
31	1476.	0.11255	71	23523.	0.04634			
32	1738.	0.10323	72	24303.	0.04558			
33	1995.	0.09652	73	24751.	0.04589			
34	2349.	0.08886	74	25213.	0.04581			
35	2602.	0.08445	75	26474.	0.04547			
36	2972.	0.07981	76	26552.	0.04523			
37	3392.	0.07521	77	26833.	0.04557			
38	3654.	0.07320	78	28269.	0.04514			
39	3912.	0.07099	79	28913.	0.04474			
40	4190.	0.06945	80	29283.	0.04472			

TABLE A10: BUNDLE P/D = 1.10 H/D = 8.3

	Re	λ		Re	λ		Re	λ
1	94.	0.78230	46	3317.	0.05957	91	27570.	0.03317
2	114.	0.64650	47	3582.	0.05751	92	27690.	0.03277
3	132.	0.57880	48	3798.	0.05593	93	29100.	0.03288
4	159.	0.45710	49	4028.	0.05460	94	29700.	0.03267
5	163.	0.44190	50	4241.	0.05348	95	31030.	0.03263
6	189.	0.38780	51	4436.	0.05223	96	31680.	0.03228
7	205.	0.36680	52	4606.	0.05067	97	32490.	0.03234
8	215.	0.34600	53	4765.	0.05091	98	33770.	0.03222
9	226.	0.35750	54	4995.	0.05003	99	34640.	0.03205
10	235.	0.29760	55	5173.	0.04911	100	35280.	0.03199
11	242.	0.30880	56	5281.	0.04889	101	36870.	0.03181
12	248.	0.31159	57	5441.	0.04732	102	37110.	0.03170
13	262.	0.30240	58	6245.	0.04549	103	39000.	0.03143
14	268.	0.32100	59	6695.	0.04577	104	39060.	0.03156
15	288.	0.27970	60	6928.	0.04375	105	40620.	0.03129
16	290.	0.27760	61	7468.	0.04269	106	41470.	0.03113
17	311.	0.29010	62	7708.	0.04224	107	41980.	0.03124
18	328.	0.25260	63	8391.	0.04165	108	44150.	0.03098
19	366.	0.24420	64	9221.	0.04045	109	44310.	0.03097
20	405.	0.21660	65	9645.	0.03858	110	46310.	0.03073
21	446.	0.20890	66	9678.	0.03948	111	46330.	0.03068
22	508.	0.18610	67	9903.	0.03962	112	49050.	0.03046
23	584.	0.17820	68	10733.	0.03897	113	49050.	0.03048
24	658.	0.15540	69	10934.	0.03854	114	52110.	0.03021
25	701.	0.14830	70	11340.	0.03846	115	52720.	0.03008
26	743.	0.14360	71	12140.	0.03757	116	54750.	0.02998
27	816.	0.13940	72	12340.	0.03786	117	58320.	0.02964
28	885.	0.12680	73	12630.	0.03717	118	61350.	0.02942
29	915.	0.12620	74	13190.	0.03720	119	64840.	0.02924
30	975.	0.12250	75	14490.	0.03672	120	67810.	0.02907
31	1026.	0.11860	76	14630.	0.03653	121	70400.	0.02884
32	1064.	0.11420	77	16090.	0.03590	122	72400.	0.02870
33	1159.	0.10820	78	16640.	0.03542	123	76099.	0.02839
34	1239.	0.10420	79	17290.	0.03543	124	79670.	0.02821
35	1323.	0.09786	80	18370.	0.03505			
36	1371.	0.09717	81	18700.	0.03497			
37	1470.	0.09512	82	20080.	0.03470			
38	1551.	0.08871	83	20690.	0.03434			
39	1600.	0.08877	84	21220.	0.03439			
40	1809.	0.08301	85	22330.	0.03420			
41	1993.	0.07892	86	23200.	0.03371			
42	2290.	0.07276	87	23520.	0.03395			
43	2547.	0.06844	88	24800.	0.03359			
44	2805.	0.06509	89	25390.	0.03329			
45	3026.	0.06220	90	26160.	0.03335			

TABLE A11: BUNDLE P/D = 1.10 H/D = 12.3

	Re	λ		Re	λ		Re	λ
1	46.	1.61670	36	2658.	0.05887	71	26480.	0.02917
2	73.	0.95850	37	2915.	0.05612	72	27070.	0.02894
3	96.	0.74279	38	3225.	0.05440	73	27780.	0.02908
4	122.	0.57210	39	3566.	0.05062	74	29510.	0.02881
5	140.	0.49840	40	3989.	0.04789	75	30280.	0.02856
6	179.	0.38470	41	4305.	0.04653	76	30830.	0.02858
7	191.	0.33440	42	4624.	0.04503	77	32100.	0.02841
8	207.	0.32430	43	4904.	0.04401	78	33420.	0.02822
9	234.	0.29970	44	4999.	0.04398	79	33750.	0.02811
10	250.	0.26120	45	5947.	0.04115	80	34650.	0.02799
11	278.	0.25650	46	7074.	0.03878	81	36100.	0.02794
12	297.	0.21600	47	7214.	0.03826	82	37410.	0.02774
13	351.	0.19870	48	7783.	0.03742	83	37520.	0.02766
14	412.	0.19020	49	8451.	0.03668	84	39020.	0.02756
15	480.	0.17500	50	9118.	0.03606	85	40250.	0.02732
16	542.	0.15620	51	9527.	0.03524	86	40910.	0.02735
17	604.	0.15490	52	9932.	0.03531	87	42930.	0.02710
18	676.	0.14730	53	10750.	0.03437	88	45590.	0.02678
19	742.	0.13710	54	11620.	0.03395	89	47860.	0.02659
20	810.	0.13140	55	12574.	0.03360	90	50510.	0.02635
21	880.	0.11950	56	12940.	0.03320	91	53180.	0.02610
22	916.	0.11530	57	14720.	0.03235	92	56810.	0.02583
23	944.	0.11450	58	14730.	0.03216	93	59520.	0.02564
24	1014.	0.10840	59	15840.	0.03198	94	59560.	0.02560
25	1092.	0.10200	60	17300.	0.03146	95	61870.	0.02547
26	1094.	0.10340	61	17560.	0.03098	96	64420.	0.02516
27	1147.	0.10020	62	18730.	0.03099	97	68798.	0.02497
28	1235.	0.09461	63	19720.	0.03070	98	71874.	0.02475
29	1309.	0.09221	64	20390.	0.03026			
30	1348.	0.08866	65	21040.	0.03034			
31	1399.	0.08790	66	22580.	0.03002			
32	1554.	0.08203	67	23590.	0.02977			
33	1796.	0.07444	68	24110.	0.02942			
34	2092.	0.06823	69	24910.	0.02957			
35	2393.	0.06241	70	25620.	0.02941			

TABLE A12: BUNDLE P/D = 1.10 H/D = 16.6